The anaerobic corrosion of carbon steel and cast iron in artificial groundwaters

N R Smart, AEA Technology plc, Culham Science Centre
D J Blackwood, National University of Singapore
L Werme, Svensk Kärnbränslehantering AB

July 2001

SKB

The anaerobic corrosion of carbon steel and cast iron in artificial groundwaters

N R Smart, AEA Technology plc, Culham Science Centre
D J Blackwood, National University of Singapore
L Werme, Svensk Kärnbränslehantering AB

July 2001

Abstract

In Sweden, high level radioactive waste will be disposed of in a canister with a copper outer and a cast iron or carbon steel inner. If the iron insert comes into contact with anoxic geological water, anaerobic corrosion leading to the generation of hydrogen will occur. This paper presents a study of the anaerobic corrosion of carbon steel and cast iron in artificial Swedish granitic groundwaters. Electrochemical methods and gas collection techniques were used to assess the mechanisms and rates of corrosion and the associated hydrogen gas production over a range of conditions. The corrosion rate is high initially but is anodically limited by the slow formation of a duplex magnetite film. The effects of key environmental parameters such as temperature and ionic strength on the anaerobic corrosion rate are discussed.

Contents

Introduction

Sweden has 12 nuclear reactors in operation at four different sites. These reactors produce about 50% of all the electricity used in Sweden. By 2010 the current nuclear programme will have produced approximately 8000 metric tons of spent nuclear fuel. After 30 to 40 years of storage in the intermediate storage facility, CLAB, the fuel will be encapsulated in corrosion resistant disposal containers. After encapsulation, the fuel will be transported to a geological repository, where the containers will be deposited at a depth of 500 to 700 m in granitic rock and surrounded by a bentonite clay backfill material.

Over a period of more than 15 years, an extensive database on groundwater chemistry has been built up. Despite the fact that the data represent widely spread geographic regions of Sweden, they present a relatively consistent picture. Groundwater in granitic rock in Sweden is oxygen-free and reducing below a depth of 100 to 200 meters. The redox potential below this depth ranges between –200 and –300 mV on the hydrogen scale and the water has a pH ranging from neutral to mildly alkaline /Smellie et al 1991 and Smellie et al 1995/.

Resistance to corrosion can be achieved in several ways. SKB has decided to approach the long-term corrosion problem by choosing a container material that is as close as possible to being immune to corrosion under the expected repository conditions. Copper has a wide stability range in oxygen-free water /Brookins 1988/ and oxygen-free conditions are expected during most of the repository performance lifetime. Dissolved sulphides in the groundwater change the situation, and copper can then corrode by formation of copper sulphide and hydrogen. The concentrations of dissolved sulphide in the near field of the canister are, however, very low and the corrosion attack on copper will, during long periods of time, be controlled by the availability of dissolved sulphides.

Pure copper does not have sufficient mechanical strength to withstand the external over-pressure of about 14 MPa at the disposal level in the repository. This pressure is composed of a water pressure of 7 MPa, corresponding to a depth of 700m, and 7 MPa swelling pressure from the bentonite. A cast iron or carbon steel insert in the container is, therefore, used to give the waste package the sufficient mechanical strength, as Figure 1 shows.

If, or when the copper corrosion shield fails, the iron insert will be in contact with oxygen-free water and hydrogen-producing, anaerobic corrosion will start. Even though the copper shell may be penetrated, the container can still act as an important barrier to the release of radionuclides from the irradiated fuel as long as the container has not collapsed. The time during which the failed container will resist the outer overpressure will depend on the corrosion rate of the iron insert. Furthermore, the hydrogen-producing anaerobic corrosion will result in an environment inside the container that may delay or prevent the release of redox sensitive toxic elements such as plutonium. Hydrogen may interact with the surrounding matrix and will eventually permeate out of the repository. Reliable long-term data for the anaerobic corrosion of iron under repository conditions are, therefore, of fundamental importance for the performance assessment of a repository for spent nuclear fuel.

Figure 1. *Exploded view of SKB canister for spent nuclear fuel.*

If the inner containers encounter trapped air, they will first be subject to aerobic corrosion, according to the following equation:

$$4Fe + 6H_2O + 3O_2 \Rightarrow 4Fe(OH)_3 \quad \text{(or a ferric salt)} \tag{1}$$

Any residual oxygen or oxidising radiolysis products will be rapidly consumed and the canister surface will become effectively anoxic /Marsh et al 1986/ and the main corrosion reaction will become:

$$Fe + 2H_2O \Rightarrow Fe(OH)_2 + H_2\uparrow \quad \text{(or a ferrous salt)} \tag{2}$$
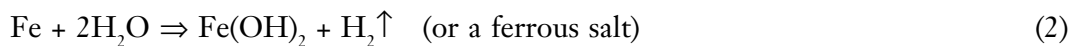
The $Fe(OH)_2$ may undergo the Schikorr reaction to produce Fe_3O_4, as follows:

$$3Fe(OH)_2 \Rightarrow Fe_3O_4 + 2H_2O + H_2\uparrow \tag{3}$$

This reaction occurs at temperatures greater than 50–60°C /Linnenbom 1958/. This paper presents an experimental study of the anaerobic corrosion of carbon steel and cast iron in artificial Swedish granitic groundwaters. The corrosion mechanisms were studied by applying a range of electrochemical techniques, both with and without an applied hydrogen overpressure. The rates of anaerobic corrosion were measured by weight loss, over a range of hydrogen overpressures, and by collection of hydrogen at atmospheric pressure. Selected samples of corrosion product were characterised using X-ray diffraction.

Experimental procedures

Materials

BS4360 grade 43A carbon steel was used in sheet and wire form. Carbon steel wires (BS4360 grade 43A) of 1 mm diameter were obtained from Winterbottom (Wiredrawers) Ltd. Cast iron test specimens measuring $150 \times 20 \times 2$ mm were supplied by Cast Metals Development Ltd. The compositions of the carbon steel and cast iron used in the experiments are shown in Table 1.

The compositions of the artificial groundwaters used in the experiments are shown in Table 2. All chemicals were analytical grade or equivalent and solutions were prepared using double-distilled water. Initial experiments were performed in a low ionic strength groundwater (KBS TR 36, Table 2), but subsequent site investigations showed that the ionic content of the groundwater could be significantly higher and so Äspö groundwater, shown in Table 2, was used for later experiments. Geochemical assessment of the Äspö groundwater showed that an atmosphere containing approximately 0.03% CO_2 was required for the solution to be stable with respect to calcite formation. Consequently a mixture of 0.03% CO_2 in nitrogen was used for deoxygenating the groundwater and for the atmosphere inside test cells, resulting in a pH below pH 7.9.

Bentonite backfill around the waste canisters will dominate the water chemistry for approximately 100,000 years after repository closure. Bentonite will remove Ca^{2+} ions from the groundwater, due to ion exchange processes involving Na^+ ions, and the pH of the solution in contact with the canister will increase from pH 8 to pH 10.5. The composition of artificial bentonite-equilibrated groundwater is given in Table 2. Earlier tests suggested that potassium sulphate led to an increase in the long-term corrosion rate and so the effect of sulphate was investigated using bentonite-equilibrated groundwater with sulphate added at a concentration of 0.1M. Geochemical calculations showed that the bentonite-equilibrated groundwater was stable with respect to calcite formation.

Table 1.   Composition of steel and cast iron used in experiments (wt%)

Material	C	Si	Mn	S	P	Mg	Ni	Cr	Al	Fe
4360 43A wire	0.21	0.220	0.7	0.017	0.017					bal
4360 43A sheet – weight loss	0.30	0.275	0.90	0.006	0.010					
4360 43A sheet – weld material weight loss	0.27	0.261	0.86	0.006	0.009					
cast iron	3.70	2.77	0.07	<0.01	0.03	0.025	0.03	0.03	0.027	bal.

Table 2. Composition of artificial groundwaters used in experiments (mM)

Ion	KBS TR 36	Äspö	Bentonite-equilibrated	Water used for weight loss tests in autoclaves
Na^+	2.84	131.3	560	6
K^+	0.10	0.19	0	
Ca^{2+}	0.45	109.5	0	1.5
Mg^{2+}	0.18	2.06	0	1.26
Cl^-	1.96	339.6	540	3
Total carbonate	2.00	0.180	10	5.63
SO_4^{2-}	0.10	7.40	0	
SiO_2	0.21			0.5
pH	8.1*	$7.0 \rightarrow 8.0$	10.5*	9.4

* Adjusted where necessary with HCl or NaOH.
The Äspö water is stabilised by maintaining a 0.03% CO_2 gas purge.
The data given above are based on the mass of chemicals added to the test solutions. Any apparent charge imbalance would be balanced by hydrolysis reactions.

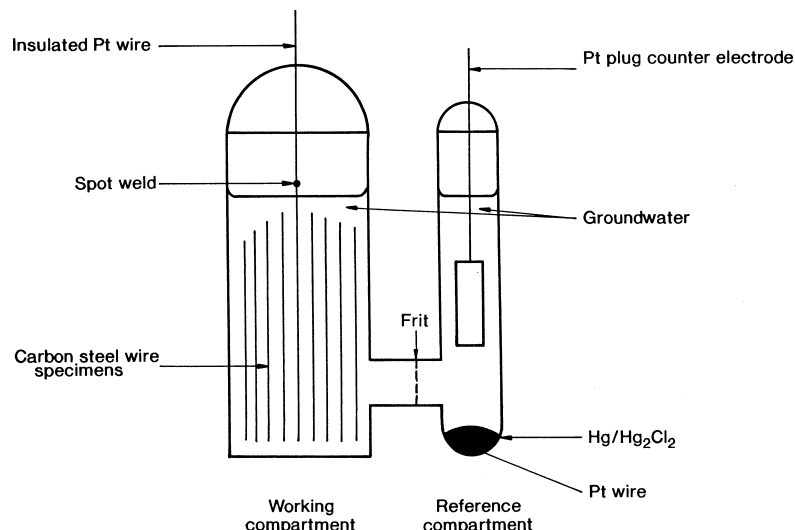## Electrochemical measurements – Atmospheric pressure

The following electrochemical measurements were conducted at atmospheric pressure:

- Open circuit potential and Tafel slopes on static wire electrodes

- Polarisation curves, cyclic voltammetry and Tafel slopes for carbon steel in oxic and anoxic groundwater, using a rotating disc electrode to examine mass transport effects.

- Scratching electrode experiments, to investigate how rapidly the film reformed on a bare metal surface.

All electrochemical potentials are quoted versus the saturated calomel electrode (SCE).

Static electrodes

The open circuit potential was measured in an H-shaped cell, of the type shown in Figure 2. The working electrode compartment of the cell contained approximately twenty carbon steel wires (~70 mm long, 1 mm diameter). The open-circuit potential of carbon steel was determined in anoxic KBS TR 36 groundwater at room temperature and at 50°C. The cell was heated by immersing it in a temperature-controlled water bath. The electrodes were tested either with a pre-existing magnetite film or after pickling in 10% HCl for 5 minutes, followed by washing in distilled water and ethanol. The coated specimens were prepared by placing the carbon steel wires in a boiling mixture of 25 wt% NaOH and 25 wt% $NaNO_3$, using the method described by Nomura and Ujihira /Nomura et al 1984/, followed by immersion in dilute artificial granitic groundwater under anoxic conditions for 3000 hours at 50°C before use (the samples were taken from a gas generation experiment).

Figure 2. *Schematic of the H-shape cells used to make electrochemical measurements on carbon steel in anaerobic granitic groundwaters. The cell was divided into two compartments; working and reference.*

Tafel slopes for carbon steel, with and without a surface layer of magnetite, were measured using the same cell as that used for the open circuit potential measurements, but only a single carbon steel wire was present in the working electrode compartment. The experiments were performed in a nitrogen-purged glove box (gaseous oxygen concentration ~4 ppm) at approximately 20°C. Under these conditions the pHs of most carbonate-bearing groundwaters are unstable, and so 0.1 M NaCl, adjusted to pH 7.5 with NaOH, was used as the electrolyte. The Tafel slopes were measured by stepping the potential to the value of interest, in 25 mV steps, and waiting for the current to stabilise, normally after 1–2 minutes.

Rotating disc electrodes

A one litre 'Pyrex' multi-necked vessel was used for the rotating disc experiments, which used a 12.7 mm diameter disc of carbon steel. To reduce oxygen diffusion into the cell the rotating disc electrode passed through a water-lock rotating seal. The working electrode connection was made via rotating carbon brush contacts. The cell contained a platinum counter electrode and a saturated calomel reference electrode connected via a Luggin probe that had a porous zirconia tip and contained 0.1M $NaHCO_3$ electrolyte. To reduce electrical noise the test cell and potentiostat were placed inside an earthed steel cabinet that served as a Faraday cage. Stainless steel gas lines and compression couplings were used for the purge gases, which were high purity nitrogen (99.999%) and commercial grade mixtures of hydrogen in argon (2.5% or 4% H_2). The gases were passed through a BASF R3-11 catalyst column operating at 400°C to remove traces of oxygen. The rotating disc assembly was placed inside a PVC bag that was continuously purged with pure argon, to provide a second barrier to atmospheric oxygen contamination. Solutions were purged with nitrogen for at least twelve hours prior to the tests and the degree of deaeration was determined by monitoring the oxygen concentration of the outlet gas using an 'Orbisphere' gas phase analyser. The outlet oxygen concentration from a typical test cell was of the order of 25 ppm or less, which corresponds to approximately 1 ppb dissolved oxygen in solution, assuming a Henry's law constant, K, of 2.95 × 10 /Turnbull et all 1987/. The temperature of the cell was maintained at 25°C throughout the test by a thermostatically controlled heating tape.

Polarisation curves were measured for BS 4630 type 43A carbon / manganese steel rotating disc electrodes in 0.01 M sodium hydrogen carbonate, which, when freshly prepared, had a pH of 8.5–9.0. The measurements were made by firstly holding the electrode at potential of –1.2V for 1000s, then stepping to the potential of interest and holding for 4000s prior to measurement of the current. Polarisation curves were determined at 10 mV intervals from -920 mV to –550 mV SCE, at rotational speeds ranging from 0 to 10 Hz. The open-circuit potential, oxygen concentration and solution pH were measured at the beginning and end of each experiment.

Cyclic voltammograms for carbon steel in both normal and 'bicarbonate-free' artificial KBS TR 36 groundwater were recorded at 20 mV sec^{-1} under both aerated and anoxic conditions.

## Zero resistance amperometry (ZRA) measurements

If the rate controlling step for anaerobic corrosion is hydrogen diffusion through a corrosion product film, the effect of connecting a platinum electrode to the carbon steel should depend on whether the film formed is ferrous hydroxide or magnetite based, because the platinum will act as a cathode and hydrogen will no longer have to diffuse through the oxide film. A series of experiments were carried out using static coupled steel and platinum electrodes. The solutions and electrode materials were the same as for the polarisation curve experiments. Cylindrical carbon steel electrodes were surrounded by platinum gauze electrodes. The temperature was maintained at either 25°C or 60°C using an external heating jacket. The solution was deaerated overnight with either nitrogen or a commercial grade hydrogen / argon mixture (2.5% or 4%), prior to insertion of the steel electrode. The cell was then further purged until a steady outlet oxygen concentration of less than 25 ppm was obtained. The purge was then moved from the solution to the gas space, to avoid agitation of the solution, and the carbon steel and platinum foil electrodes were connected via a zero resistance ammeter. The couple potential and galvanic current were recorded. The duration of the experiments was typically of the order of seven days, but they were terminated at shorter times if the potentials moved above –600 mV SCE. The open-circuit potential, oxygen concentration and solution pH were measured at the beginning and end of each experiment.

Scratching electrode

The aim of these experiments was to investigate the stability of the iron hydroxide/magnetite films formed under anoxic conditions. The electrode surface was scratched in-situ by a diamond stylus using a rotating disc scratching electrode assembly (Figure 3). The rotation rate was 10 Hz and the ratio of scratched surface area per revolution to the total surface area of the electrode was approximately 1:200. All experiments were carried out on a carbon steel disc electrode, type BS4360 grade 43A, with an area of 0.8 cm^2, ground to a 600 grit finish. The test solution was initially the artificial groundwater given in Table 2, but in later experiments the bicarbonate component was omitted, to avoid pH drift.

Electrochemical measurements with hydrogen overpressure

Corrosion potential and Tafel slope measurements were performed in autoclaves to assess the effect of hydrogen overpressure on the kinetics of the anaerobic corrosion reaction. Three electrode cells were prepared in lidded cylindrical PTFE vessels. Each cell contained a BS4360 43A forged carbon steel coupon working electrode, a platinum foil counter electrode, and a calomel reference electrode. Argon-purged 3.5% NaCl solution was introduced into the cells inside an argon filled glovebox, and the assembly was placed in a steel autoclave. After sealing, the autoclaves were removed from the glovebox. In some
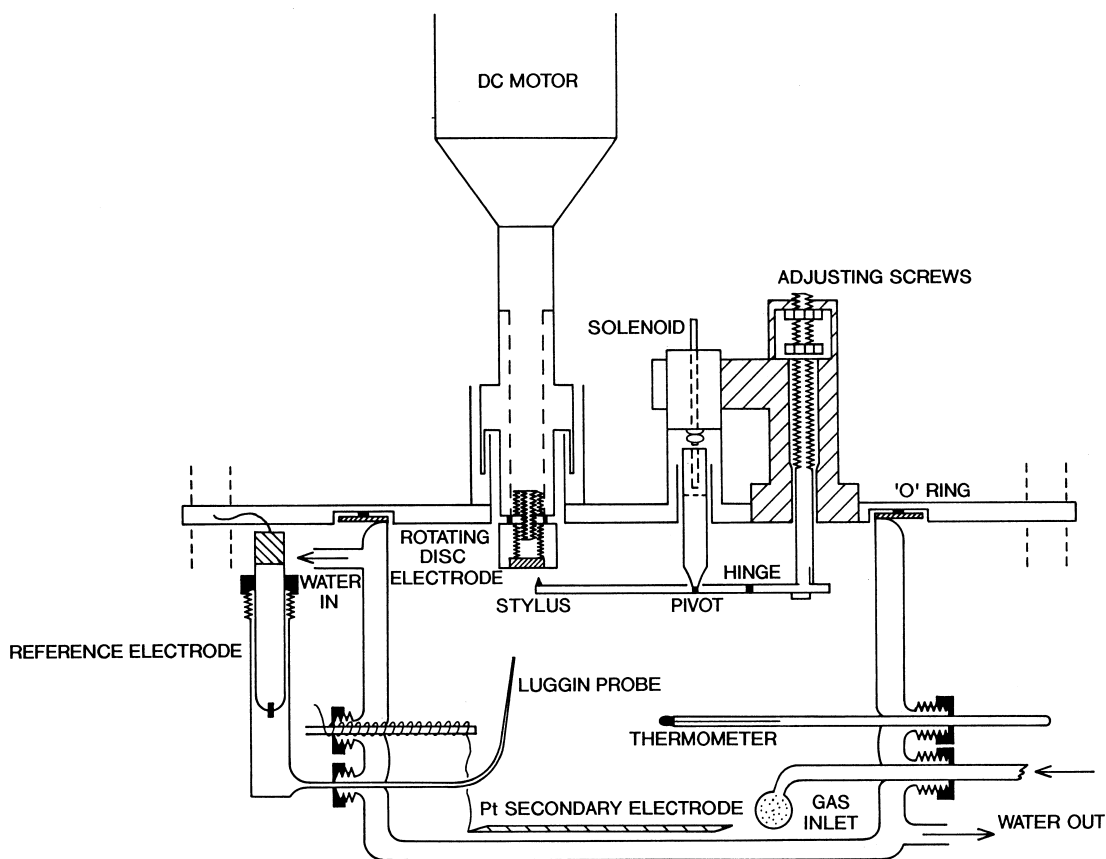
Figure 3. *Scratching electrode rotating disc assembly*

experiments the autoclaves were filled with hydrogen to the required overpressure. In later tests the electrolyte was pre-saturated with hydrogen before adding it to the cell. After allowing the rest potential (E_{rest}) to stabilise, cyclic voltammetry was performed at a scan rate of 0.2 mV/s, to a cut-off current of 1.2 mA/cm^2. The Tafel regions of the resulting cathodic and anodic polarisation curves were analysed to generate Tafel constants.

Weight loss with hydrogen overpressure

Long-term immersion tests were undertaken to investigate the effect of hydrogen over-pressure on the anaerobic corrosion of carbon steel. Coupons with dimensions of 50 × 30 × 1 mm were prepared from two carbon steel blocks, one of which had been exposed to a full penetration autogenous electron beam weld. Specimens were cut from the welded block so that the weld was in the centre of each coupon. There were only slight compositional differences between the plain and welded areas (Table 1). Six plain and six welded pre-weighed coupons were assembled in PTFE racks and positioned inside cylindrical PTFE pots. Each vessel was then filled with artificial groundwater (Table 2). Three of the filled PTFE pots were assembled into separate steel autoclaves and the lids sealed into position. The dissolved air was replaced by argon and then hydrogen, and finally each autoclave was brought up to its operating pressure of either 1, 10 or 100 atms of hydrogen (0.1, 1 or 10 MPa). The autoclaves were then placed in a thermostatically controlled oil bath at 90°C. The tests lasted for up to four years.

After appropriate exposure times coupons were removed from each autoclave and their corrosion rates determined by weight loss measurement. The remaining coupons were immediately returned to their respective autoclaves, and refilled with hydrogen. For the

coupons that had been exposed for 120 and 343 days the corrected weight loss due to corrosion was determined by double immersion in Clarke's solution (folowing ASTM G1-90), but a refined method, using linear regression analysis of the weight losses after 2.5, 5, 10 and 20 minutes immersion in Clarke's solution, was applied to samples exposed for longer periods. Correlation coefficients for the linear regression were usually better than 0.998. The corrosion products on selected specimens were characterised using X-ray diffraction.

Gas evolution measurements

The anaerobic corrosion rates of carbon steel in various artificial groundwaters were measured by measuring the rate of hydrogen evolution, using the barometric cell designs shown in Figure 4. Before assembly, all the cell components were degreased in methylated spirits, rinsed in distilled water and dried. The cell components (except for the precision bore tube (pbt)) were then transferred to an inert gas glovebox with a residual oxygen level of less than 5 ppm, where the cells were assembled. The cells contained 50 mm lengths of BS4360 grade 43A carbon steel wire, or coupons of cast iron, with a total surface area of ~0.1 m². The Dreschel bottle reservoir was filled with di-n-butyl phthalate (DBP, a low vapour pressure liquid) and the glass joints were sealed with epoxy resin. The valves were then closed, the assembly was removed from the glovebox and the precision bore tube sealed in place with epoxy resin. Finally a layer of silicone sealant was applied to the exposed 'Araldite' to protect the epoxy from degradation in the water bath. The cell was evacuated and backfilled with hydrogen three times. A hydrogen atmosphere was retained in the cell. Initial attempts to measure the rate of hydrogen gas production at 80°C were unsuccessful because the DBP was hydrolysed by the water vapour. The cell design was therefore modified to use mercury instead of DBP (Figure 4 (b)). The test cell temperature was controlled by immersion in a thermostatically controlled oil bath or water bath.
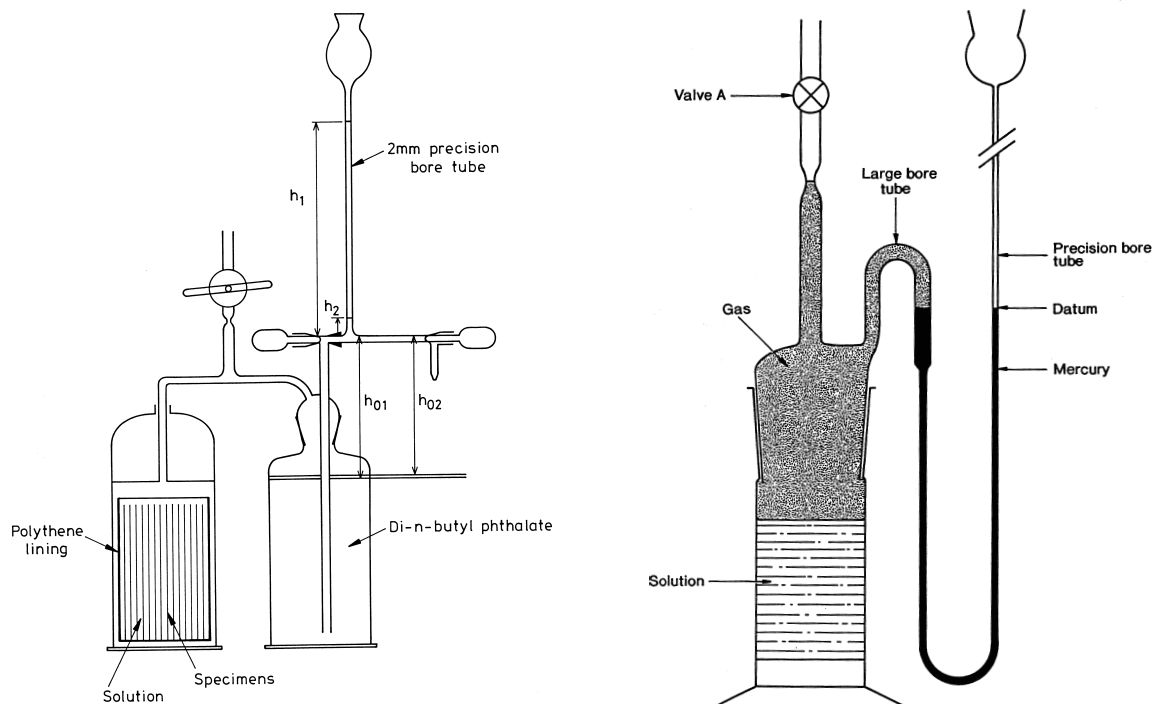
Figure 4. *Schematic diagram of the cells used to determine hydrogen evolution rates at (a) 30 and 50°C, (b) 85°C.*

14

When corrosion occurred the hydrogen produced caused the liquid level in the manometer tube to rise and the new volume of hydrogen in the cell was determined from the height of the manometer liquid. Hence the volume of hydrogen (DV) produced by corrosion was calculated. The results were corrected for the external atmospheric pressure. Hydrogen evolution rates could be determined to within ± 0.5 dm^3 (STP) m^{-2} year^{-1}. Control cells, without any corroding steel, were also set up. A number of experimental parameters were investigated using the gas cell technique; a summary of the test conditions is given in Table 3 and details are given below.

Effect of water immersion

Comparative tests were carried out under high humidity, partial immersion and full immersion conditions, by using gas evolution cells with the following arrangements:

- Carbon steel wires fully immersed in artificial KBS TR 36 groundwater;

- Carbon steel wires positioned completely clear of a reservoir of artificial KBS TR 36 groundwater;

- Carbon steel wires dipped in KBS TR 36 groundwater so that approximately 20% of their surface area was in direct contact with the solution.

Effect of surface treatment

In order to measure the maximum likely hydrogen evolution rate the air-formed oxide film in most experiments was removed by pickling the wire samples before they were placed in the barometric cells. The procedure for pickling was to degrease the wires with alcohol, then pickle them in 10% HCl for 5 minutes, followed by three washings in clean double-distilled water to remove any residual acid and finally a rinse with absolute ethanol.

Table 3. Summary of experimental conditions for gas cell experiments

Water	Temperature	Surface treatment
Swedish granitic GW - KBS TR 36	30	pickled
	30	degreased
	50	pickled
	50	degreased
saturated water vapour – partially immersed and fully in vapour	50	pickled
with magnetite and carbonate films previously formed	50	
with 0.1M FeSO$_4$ and 0.1M K$_2$SO$_4$ additions	50	pickled
NH$_3$ addition	50	pickled
HNO$_3$ addition	50	pickled
10′ ionic strength		
Äspö groundwater	50	pickled
Bentonite-equilibrated groundwater	50	pickled
Bentonite-equilibrated + sulphate	50	pickled
Äspö groundwater	50	cast iron
Bentonite-equilibrated groundwater	50	cast iron
Äspö groundwater	85	cast iron and carbon steel

To investigate the effect of pre-existing air-formed oxide films on the rate of corrosion, some specimens were tested after a simple degreasing procedure in absolute alcohol. To study the effects of other possible corrosion products on the corrosion rate, tests were also carried out using carbon steel wires with pre-formed films of either iron(II) carbonate or magnetite. Magnetite films were grown using the method described by Nomura and Ujihira /Nomura et al 1984/. Carbonate films were formed by placing the carbon steel in a solution of artificial groundwater which was continuously purged with carbon dioxide for one to thirty days, at 50ºC.

Effect of dissolved ferrous ion concentration

If the long-term corrosion rate of carbon steel under anaerobic conditions is restricted by the formation of a protective film, the rate at which the film forms could depend on the concentration of Fe^{2+} ions in the surrounding solution. To test this effect, hydrogen evolution experiments were conducted with carbon steel immersed in KBS TR36 groundwater that contained 0.1M $FeSO_4$ or which was saturated with $FeCO_3$.

Effect of radiolysis products

Ammonia and nitric acid are possible radiolysis products from water vapour and nitrogen. Both species may influence the corrosion rate and so experiments were conducted with KBS TR36 groundwater containing 9 mM NH_3 or 3 mM HNO_3. These are predicted to be the maximum concentrations inside the canister annulus.

Ionic strength

The effect of ionic strength on the rate of hydrogen evolution was investigated using a solution containing 10× the ionic concentrations of KBS TR36 artificial groundwater. The pH was adjusted to 8.1 with HCl.

Effect of groundwater composition

Gas generation rates were measured in three artificial groundwaters, as shown in Table 2.

Effect of temperature

Gas generation rates were measured at 30°C, 50°C and 85°C.

Effect of removing corrosion product

The effect of removing loosely adhering corrosion product was investigated using carbon steel wire which had been anaerobically corroded in KBS TR36 artificial groundwater for approximately two years at 50°C. The loose corrosion product was removed from the surface by wiping with tissue paper, inside an inert gas glove box. Copious quantities of corrosion product were removed, but a layer of black adherent corrosion product remained on the surface. The cleaned carbon steel wires were then placed in a new gas cell, immersed in fresh deaerated KBS TR36 groundwater and reheated to 50°C.

Comparison of cast iron and carbon steel

Gas generation rates were measured for cast iron in Äspö water at 50°C and 85°C, for comparison with carbon steel corroded in the same waters.

Results

Electrochemical measurements – atmospheric pressure

Open circuit potential

The potentials (mV vs SCE) of the pickled mild steel in KBS TR36 groundwater, at room temperature and at 50°C, were approximately –760 and –815 mV respectively. For the unpickled specimens (i.e. those with a surface oxide present) the potentials were –745 mV at room temperature and –795 mV at 50°C. As a corrosion product film developed on the pickled carbon steel electrode a positive shift in its open-circuit potential occurred and it converged with that of the unpickled specimen after around 700 hours. The groundwater was at pH 8.1 ± 0.1 throughout the course of the experiment.

Tafel slopes – static electrodes

Figure 5 shows Tafel plots obtained from pickled carbon steel specimens, and carbon steel specimens coated with a magnetite film by the Nomura method. The pickled carbon steel specimen exhibited an anodic Tafel slope of 62.5 mV decade^{-1}, a corrosion current density (I_c) of 2.1 μ/A cm^{-2} and a corrosion potential (E_c) of about –790 mV vs SCE. These values are in good agreement with data in the literature /Turnbull et al 1982; Turnbull et al 1987/ and are consistent with the anodic dissolution reaction:

$$Fe \rightarrow Fe^{2+} + 2e^{-} \tag{4}$$
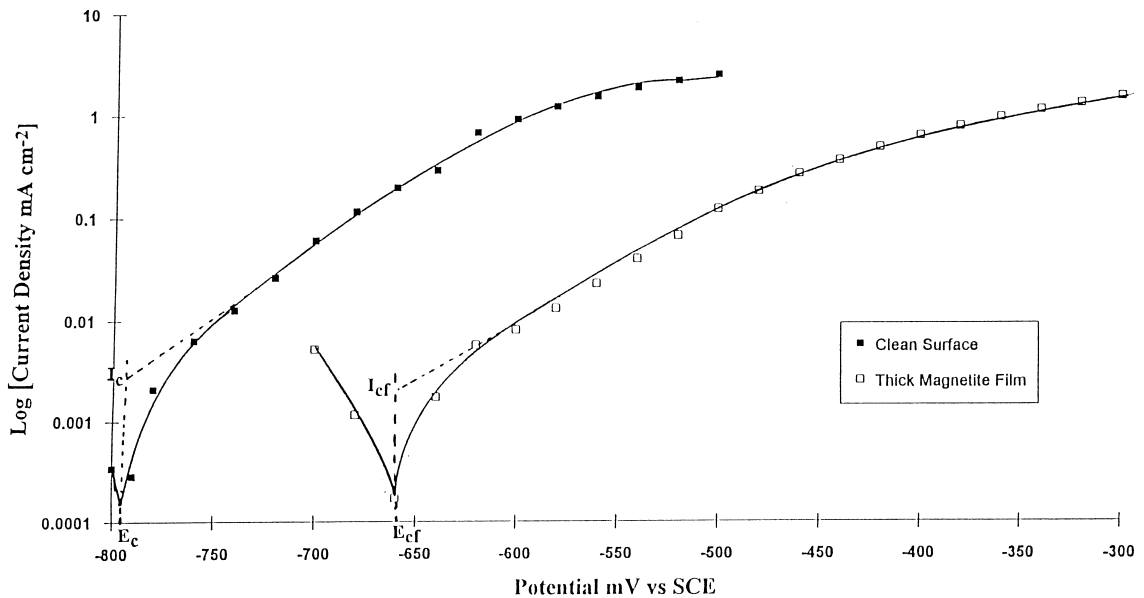

Figure 5. *Tafel plots obtained from carbon steel electrodes, with and without a magnetite film, in 0.1 M NaCl adjusted to pH 7.7. E_c and I_c are the corrosion potential and corrosion current for a carbon steel electode without a magnetite film repectively. E_{cf} and I_{cf} are the corresponding parameters for a carbon steel electode covered with a magnetite film.*

The corrosion current density for an 'oxide free' carbon steel specimen of 2.1 μA cm^{-2} is equivalent to a corrosion rate of ~23 μm year^{-1}. At potentials positive of –600 mV vs SCE the Tafel plot shows that the carbon steel started to form a passive film, which probably consisted of $Fe(OH)_3$ or Fe_2O_3. The presence of an existing magnetite film resulted in the value of the Tafel slope increasing to 74.1 mV dec^{-1}, the corrosion current density (Icf) decreasing to 0.7 μA cm^{-2} and the corrosion potential (Ecf) shifting positively to about -670 mV vs SCE. This value is slightly positive of the water reduction potential at pH 7.5, which is –683 mV vs SCE. The corrosion current density for a magnetite covered carbon steel specimen of 0.7 μA cm^{-2} is equivalent to a corrosion rate of ~8 μm year^{-1}.

Polarisation curves – rotating disc electrode

The polarisation curves determined at various rotation frequencies in 0.01M $NaHCO_3$ (initial pH 8.5–9.0) are shown in Figure 6 and the oxygen levels and rest potentials are tabulated in Table 4. Since the bicarbonate ions in solution were in equilibrium with a low concentration of dissolved carbon dioxide a small proportion of the carbonate was lost continuously from the solution as carbon dioxide, which was carried away with the purge gas, giving rise to an increase in the solution pH. The polarisation curves indicated an active-passive transition in the region of –780 mV vs SCE. This is the potential where an FeOH film is reported to form in 1 M HCO_3^- solutions /Bockris et al 1971/. The observation of an active-passive transition confirms the results of Davies and Burstein /Davies et al 1980/. The anodic and cathodic Tafel slopes were measured from the polarisation curves in the region of the open-circuit corrosion potential (Table 4). The anodic Tafel slopes were in the region of 60 mV dec^{-1}.
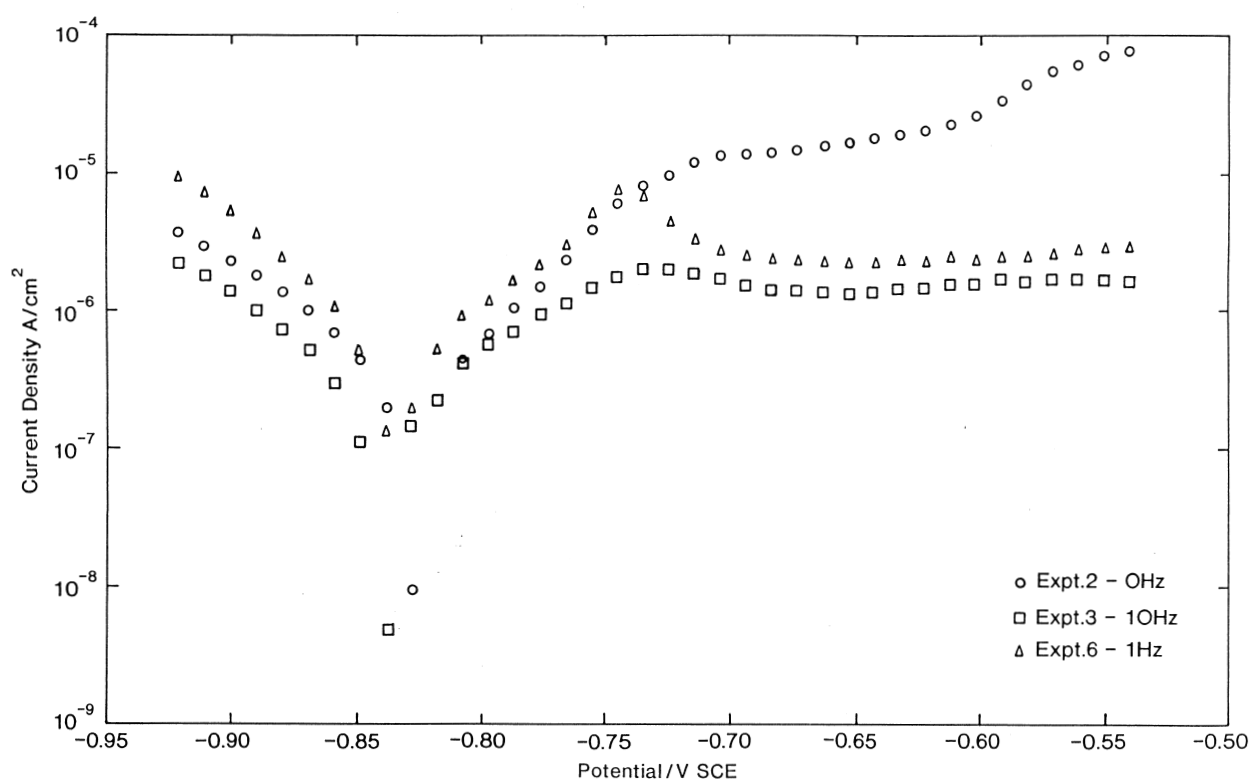
Figure 6. *Polarisation curves for carbon steel in 0.01M NaHCO₃ at various rotational frequencies.*

Table 4. Summary of potentiostatic polarisation experiments

| Disk Speed (Hz)	Conditions	pH	O_2 (ppm)	Potentials (mV vs SCE) Steel	E_c	Pt	Tafel Const. mV dec^{-1} b_a	b_c
0	N_2 purge	8.53	–	–887	–726	–820	60	–50
	30 hours	9.37	–	–912	–220	–		
1	Ar purge	8.64	19	–790	–50	–860	59	–50
	24 hours	9.57	14	–610	–540			
10	Ar purge	8.62	5.1	–776	–373	–890	63	–54
	16 hours	9.75	38	–575	–500			

A freshly polished carbon steel electrode was placed into deoxygenated 'bicarbonate-free' artificial KBS TR 36 groundwater (pH 8.1) and rotated at 10 Hz. After approximately ninety minutes, a stable open-circuit potential of -0.73 V vs SCE was obtained. Potentials between –0.72 V and –0.50 V vs SCE were then applied to the electrode and the resultant current flow after three minutes was recorded. These data enabled a pseudo-Tafel plot to be constructed (Figure 7); it had a slope close to the expected value of 60 mV dec^{-1}. The active dissolution current, i_{corr}, was 0.46 ± 0.18 μA cm^{-2}, which is equivalent to a corrosion rate of 5.4 ± 2.1 μm per year. This should be taken as an upper value, since the possibility exists that part of the measured corrosion current arises from the oxidation of some of the hydrogen in the 96% Ar / 4% H_2 mixture used to deoxygenate the system. Based on the diffusion-limited current, the maximum amount of residual oxygen in the solution was estimated to be 8 ppb. Within 5 minutes of switching the electrode back to open-circuit conditions at the end of the experiment, E_c had fallen back to –0.74V vs SCE, indicating that no effective barrier to the dissolution process had formed on the electrode surface. No oxide film was visible on the electrode surface.

Cyclic voltammetry – rotating disc electrode

The cyclic voltammograms for carbon steel in both normal and 'bicarbonate-free' artificial groundwater were similar to Figure 8, with no passive region being observed. The presence of bicarbonate or oxygen had little effect on the shape of the voltammogram. Inspection of the electrode surface after the cyclic voltammetry measurements revealed moderate pitting in all cases, but no visible corrosion product. The electrode exhibited active dissolution up to a potential of +0.2 V vs SCE. This is in reasonable agreement with Pourbaix /Pourbaix et al 1974/, who found that the onset of passivation for iron occurred above pH 8.0; the pH of the artificial groundwater was 8.1 and was therefore on the borderline between active and passive corrosion. In contrast, in the polarisation curve measurements using 0.01M NaHCO$_3$, which had a slightly higher pH (8.5–9.0), an active – passive transition was observed.

Zero resistance amperometry

The initial and final potentials and galvanic currents between the platinum-steel couples, along with the oxygen levels and other experimental parameters, are given in Table 5. As before, the pH increased during the test because of carbon dioxide removal – the effect was greater in experiments at 60°C. There was a significant difference in the behaviour of the experiments at 25°C and 60°C, which may reflect the differing propensity of the system for magnetite formation via the 'Schikorr' reaction to occur at these two tempera-
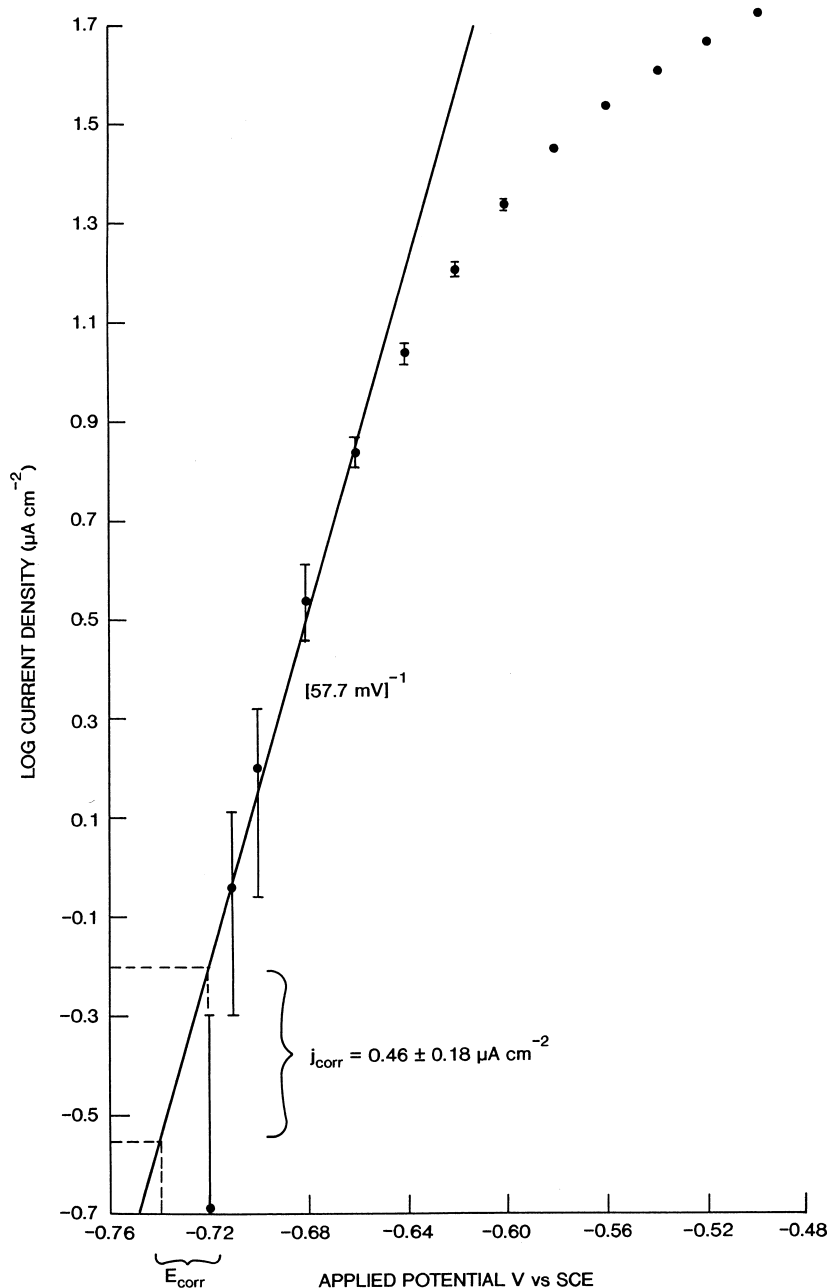
Figure 7. *Pseudo Tafel plot constructed for carbon steel in into deoxygenated 'bicarbonate-free' Swedish granitic groundwater (pH 8.1) and rotated at 10 Hz*

tures (equation 3). At 25°C, the potential of the couple typically remained at 'active' potentials (i.e. more negative than –700 mV SCE), throughout the experiments, which ran for approximately seven days. At 60°C the couple potential, though starting at active potentials, was not stable and generally drifted in a positive direction, rapidly reaching potentials consistent with the steel electrode having passivated.

The drift to passive potentials at 60°C was also observed when the purge gas was hydrogen in argon. Having achieved passive potentials the steel was typically more positive than the platinum foil. This may reflect the fact that the platinum was behaving as a hydrogen electrode, whereas the potential of the steel electrode would have been affected
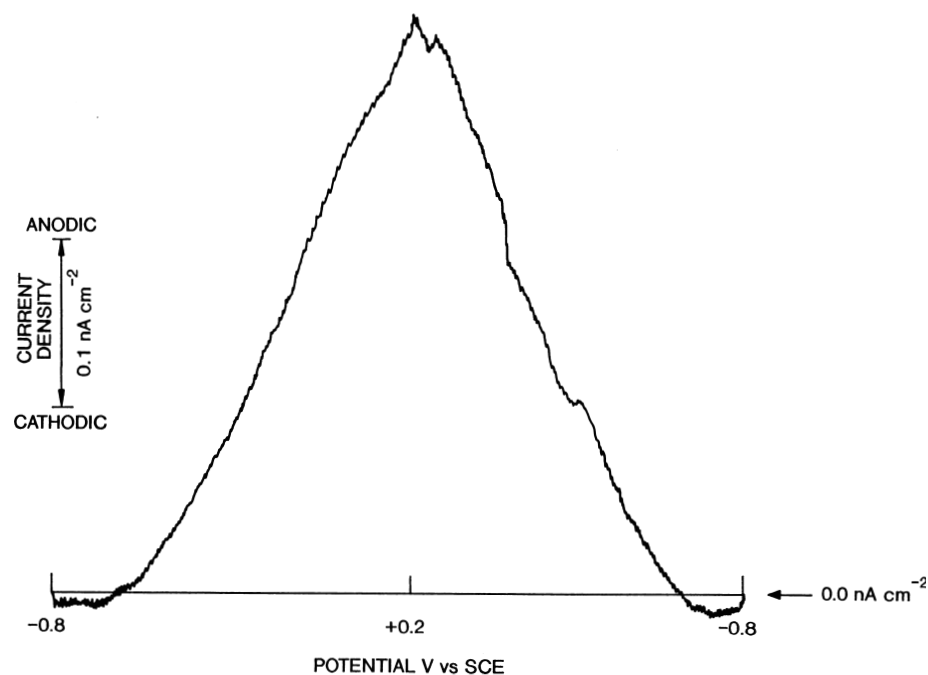
Figure 8. *Cyclic voltammogram of a carbon steel electrode in deaerated 'bicarbonate-free' artificial groundwater.*

Table 5.   Summary of ZRA experiments

Expt. Label	Purge gas	Conditions*	pH	O$_2$ (vpm)	Potentials (mV vs SCE) C steel	Pt	E$_{couple}$	Current (μA)
					Experiments at 25°C			
A	N$_2$	Purge 12 days	8.5	40	−843	−154	−808	35
		Run 7 days	10.1	24	−624	−458	−601	0.21
B	N$_2$	Purge 24 hrs	8.6	40	−792	−172	−788	0.5
		Run 5 days	9.6	40	−798	−695	−796	0.088
C	Ar 2.5% H$_2$	Purge 20 hrs	8.6	27	−1023	−930	−880	0.07
		Run 7 days	9.6	27	−779	−725	--778	0.034
D	Ar 2.5% H$_2$	Purge 24 hrs	8.6	4.8	−775	−450	−774	0.23
		Run 5 days	9.8	14	−800	−712	−798	0.057
E	Ar 4% H$_2$	Purge 24 hrs	8.5	11	−784	−726	−783	0.068
		Run 5 days	9.7	15	−799	−750	−796	0.042
					Experiments at 60°C			
F	N$_2$	Purge 4 days	8.8	8	−823	−197	−675	1.4
			10.8	18	−281	−288	−290	0.014
G	N$_2$	Purge 21 hrs.	8.6	40	−849	−175	−820	40
			10.2	33	−323	−313	−323	0.02
H	Ar 4% H$_2$	Purge 25 hrs.	8.5	11	−847	−685	−818	16
			10.2	16	−447	−666	−564	0.39

* The two rows for each experiment correspond to the conditions at the start and finish.

by the presence of an oxide on the surface of the steel. Reduction of any residual haematite would have provided a source of cathodic current and so raised the potential of the electrode.

At 25°C, with nitrogen as the purge gas, the potential of the platinum electrode when uncoupled was typically highly positive, approximately –200 mV, indicating that it was behaving as an oxygen electrode under the influence of the residual oxygen in the system. With the argon/hydrogen purge gas the platinum behaved as a hydrogen electrode, taking up a potential in the region of –720 to –780 mV, as expected from the solution pH. In contrast, the potential of the carbon steel-platinum couples was independent of the nature of the purge gas, indicating that the oxygen exchange current at the platinum electrode in the nitrogen purged solution was insufficient to support the steel corrosion process.

There was a difference in the magnitudes of the couple currents between nitrogen and argon/hydrogen purged solutions. In the hydrogen-purged solutions the final currents were generally slightly lower than in the nitrogen-purged experiments. In the nitrogen-purged experiments at 25°C the initial current was high, but subsequently decreased to a steady state current about 1–2 orders of magnitude smaller. Although this fall was initially very rapid, the steady state value was generally only achieved after two to three days. In the hydrogen/argon purged experiments the galvanic current was reasonably steady throughout (see Table 5).

Scratching electrode experiments

Aerated conditions

A carbon steel electrode placed in air-saturated groundwater (see Table 2) initially adopted a rest potential, E_c, of –0.42V vs SCE. On applying a rotation at 10 Hz, E_c rose significantly, reaching as high as –0.27 V after a period of some 10 minutes. On stopping the rotation, E_c fell slowly, taking several hours to return to its original value. These observations suggest that upon rotation the increase in the mass transport of oxygen to the electrode surface was sufficient to fully overcome the active dissolution process and thus allow a passive Fe_2O_3 film to form, hence the rise in the value of E_c. When rotation ceased, the open-circuit potential was controlled by the slow dissolution of the Fe_2O_3 film.

On most occasions, pitting occurred on the carbon steel electrode within two hours of being placed in solution, regardless of whether or not it had been rotated. The nucleation time depended on surface roughness. Pits were clearly visible to the naked eye, and were usually shallow but broad. Copious quantities of black corrosion product were also observed over the electrode surface. Pitting corrosion occurred at rates high enough to force E_c down to –0.66 V vs SCE. The decrease in potential was due to an increase in the overpotential for oxygen reduction required to compensate for the increase in the corrosion rate at the freshly exposed metal surface.

On scratching the rotating carbon steel electrodes in aerated conditions, open-circuit voltage-time transients such as that shown in Figure 9 were produced. During scratching, E_c moved in a negative direction. As soon as the stylus was removed from the electrode surface, E_c rapidly returned to its initial value, indicating that complete repassivation occurred. Repassivation occurred within a period of three minutes. Visual inspection of the scratched electrode showed minor amounts of corrosion product emanating from the scratch compared with the large amount seen previously around pits.
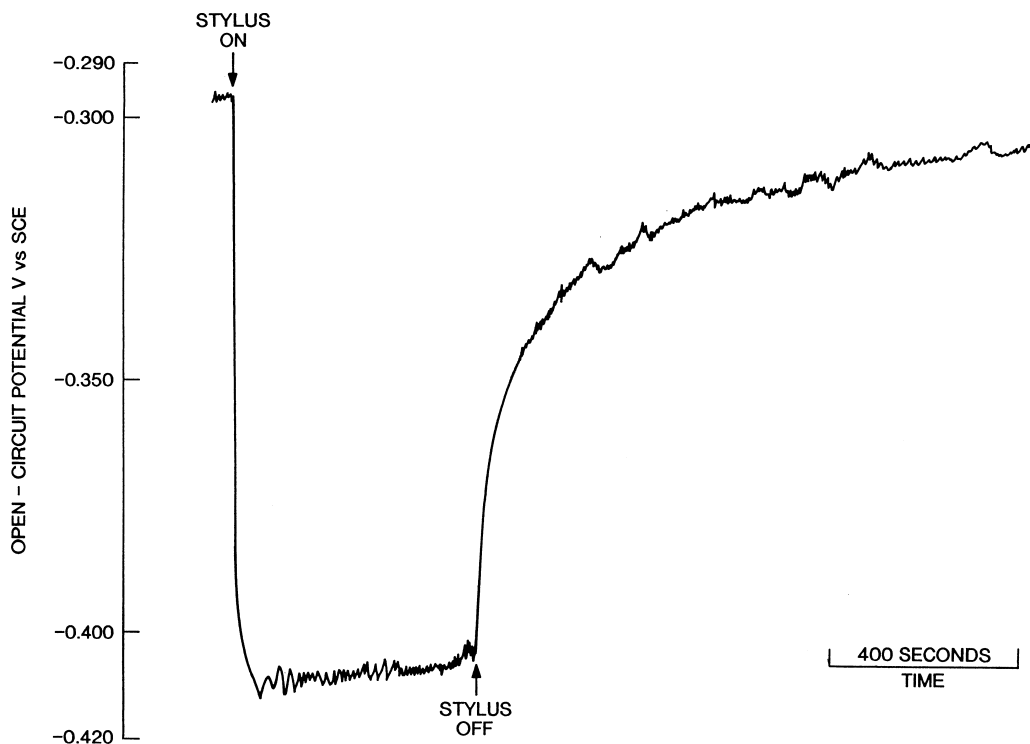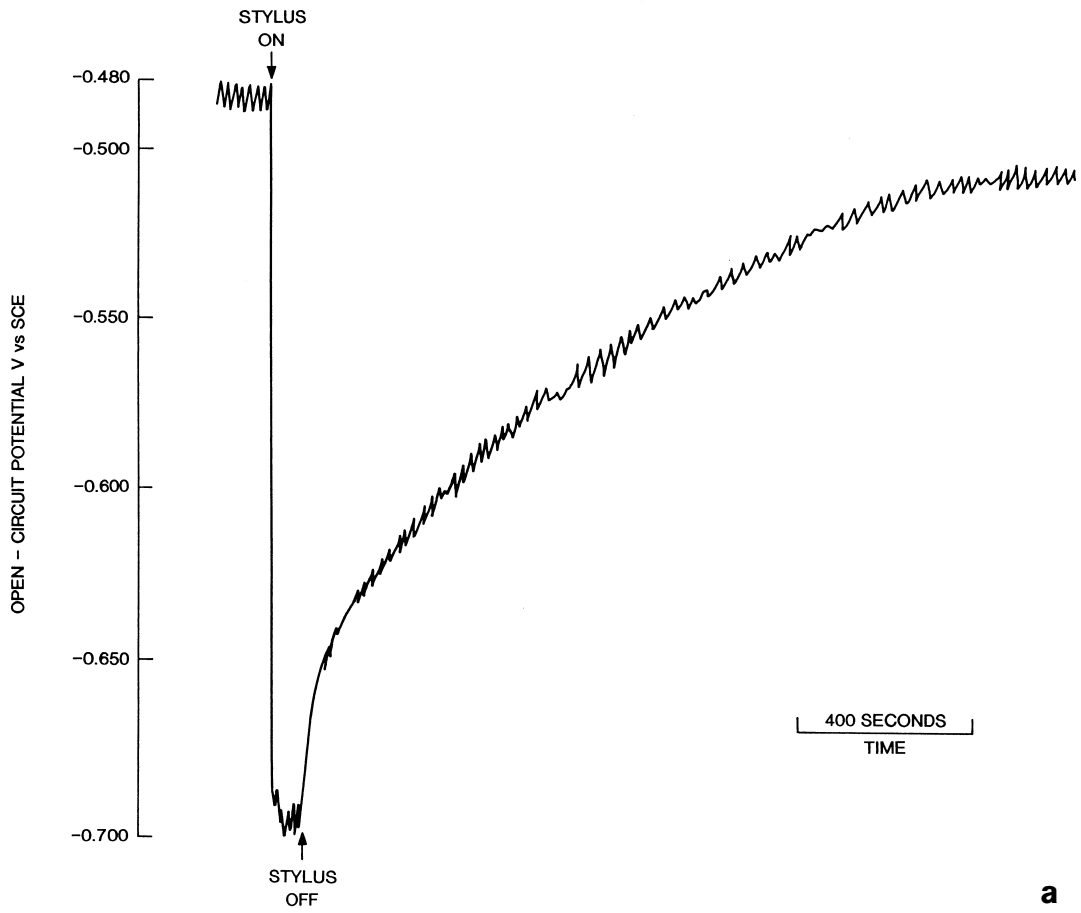
Figure 9. *Open circuit potential-time transient obtained when scratching a carbon steel electrode for 1 minute in artificial Swedish granitic groundwater under aerated conditions.*

Anoxic conditions

A freshly polished carbon steel electrode was placed in a solution of artificial groundwater (see Table 2) that had been deaerated with argon for approximately sixty minutes. The value of the electrode open-circuit potential (E_c) was initially -0.55 V vs SCE and was virtually independent of the rate of rotation. However over thirty minutes, E_c gradually increased to a new stable value of –0.48 V vs SCE, suggesting that there was some residual dissolved oxygen and an Fe_2O_3 film was able to slowly form. On scratching the carbon steel electrode for a period of one minute, E_c fell from -0.48 V to -0.70 V vs SCE (Figure 10a). When the stylus was removed E_c recovered gradually, and after 30 minutes it had reached a new steady state value of –0.52 V vs SCE. After the electrode was scratched for a second time, the open-circuit potential became positive of the hydrogen evolution potential for a relatively short period, then became more negative again (Figure 10b). Scratching the surface a third time had only a relatively small effect on the value of E_c, a drop of only a few tens of millivolts occurred whilst the stylus was in actual contact with the electrode followed by a rapid recovery upon their separation (Figure 10c).

Some difficulties were experienced in maintaining a stable pH while purging with argon, due to the removal of carbon dioxide and a shift in the position of the carbonate equilibrium, and so the experiments were repeated in solutions that did not contain bicarbonate. These solutions maintained a stable pH of 8.0 to 8.2 during argon purging. Freshly polished carbon steel electrodes attained open-circuit potentials below the hydrogen evolution potential after a period of approximately one hour, finally adopting rest potentials between –0.72 V and –0.74 V vs SCE. On scratching the surface, the potential transient shown in Figure 11 was observed. When the scratch was made, E_c fell rapidly but on removal of the stylus it took about 12 minutes to recover to its initial value. No visible oxide was observable on the electrode surface at the end of the experiments, suggesting that the film was less than a few hundred nanometres thick.

24
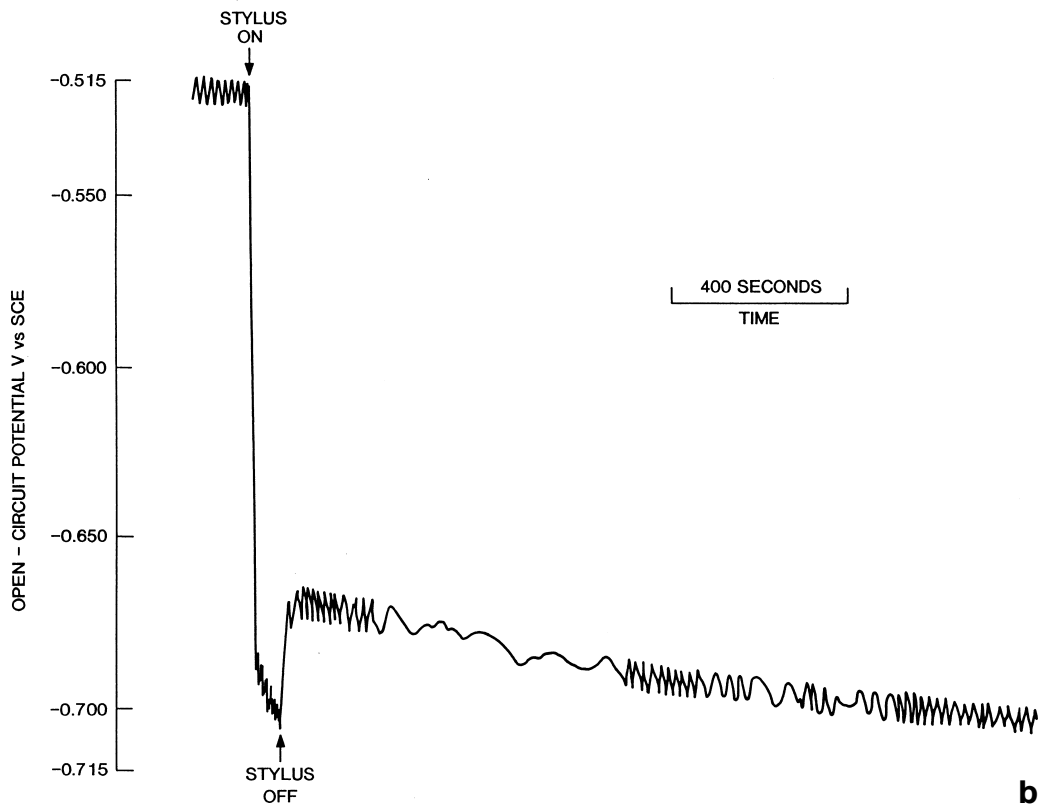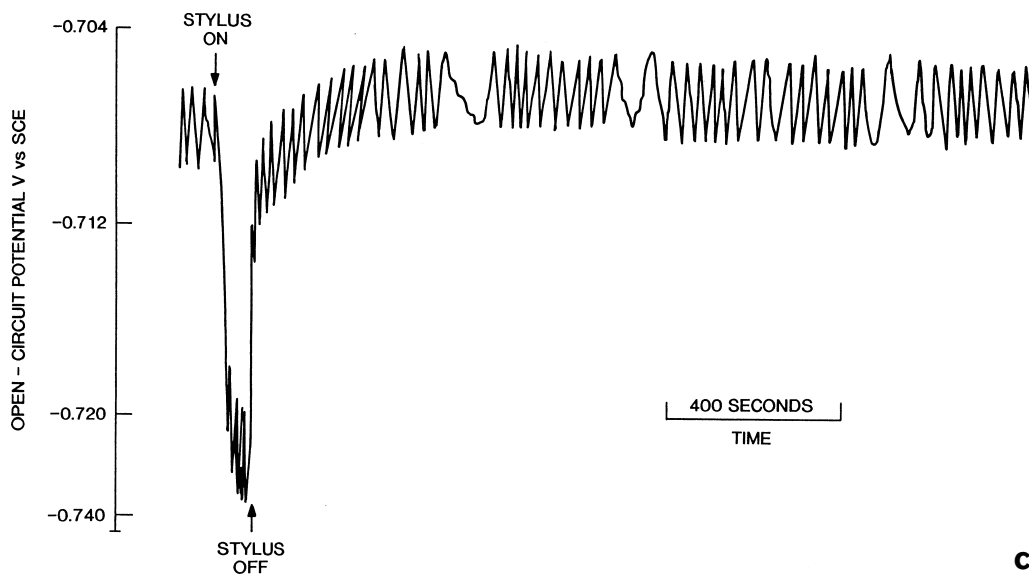
Figure 10. *Open circuit potential-time transient obtained when scratching a carbon steel electrode for 1 minute in artificial Swedish granitic groundwater purged with 96% argon / 4% hydrogen, showing three successive scratching experiments.*

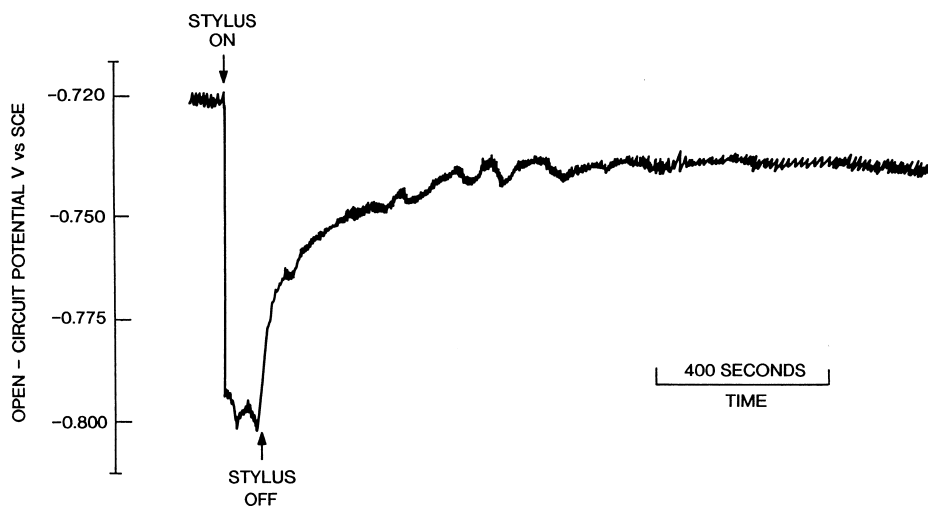**Figure 11.** *Open circuit potential-time transient obtained when scratching a carbon steel electrode for 1 minute in bicarbonate-free artificial Swedish granitic groundwater purged with 96% argon / 4% hydrogen.*

Electrochemical measurements – hydrogen overpressure

The results from the electrochemical measurements under elevated pressures are given in Table 6. Cathodic and anodic Tafel values were equated in order to estimate the corrosion potential, E_c and the corrosion current density, i_{corr}.

Weight loss – hydrogen overpressure

The results of the weight loss experiments are summarised in Table 7. The mean corrosion rates were low and generally <1 μm/year. They tended to decrease with length of exposure, which is consistent with the formation of a protective magnetite layer over the surface of the carbon steel. Welding had an insignificant effect on the anaerobic corrosion rate of carbon steel.

Characterisation of corrosion product

The coupons from the weight loss experiments took on a black mottled appearance at all three test pressures (1, 10 and 100 atm). Three coupons which had been exposed for twelve months were examined by X-ray diffraction to determine the nature of the surface film. All three showed the presence of Fe_3O_4 (magnetite) in amounts that increased in the order 1 atm < 100 atm < 10 atm. This is the same order as the corrosion rates (Table 7), showing that the higher the corrosion rate the more magnetite was produced.

Table 6.   Corrosion potentials and current densistes obtained from autoclave polarisation studies

Label	Gas	Pressure (Atms)	Temp (°C)	E_{rest} (mV/SCE)	E_c (mV/SCE)	i_{corr} (A.cm^{-2})	B_c (mV dec^{-1})	B_a (mV dec^{-1})
A	Argon	1	24	−784	−816	1.7×10^{-6}	−156	71
B	"	1	24	−778	−772	1.6×10^{-6}	−178	55
D	"	1	50	−805	−834	1.2×10^{-6}	−126	74
E	"	1	80	−825	−837	2.7×10^{-6}	−168	46
5	Hydrogen	1	24	−787	−848	1.1×10^{-6}	−132	71
6	"	1	24	−789	−712	1.3×10^{-6}	−191	55
7	"	10	24	−812	−808	3.5×10^{-6}	−199	75
9	"	85	24	−796	−768	1.4×10^{-6}	−194	59
1	Hydrogen	1	50	−801	−854	9.8×10^{-7}	−144	66
2	"	10	50	−810	−830	3.1×10^{-6}	−158	67
3	"	85	50	−807	−808	4.3×10^{-6}	−204	54
10	Hydrogen	1	80	−822	−832	2.8×10^{-6}	−161	47
11	"	10	80	−825	−829	7.2×10^{-6}	−183	52
12	"	85	80	−814	−800	1.2×10^{-5}	−149	50
4	"	84	80	−827	−837	7.9×10^{-6}	−188	57
*13	Hydrogen	10	25	−777	−774	3.5×10^{-7}	−180	49
*14	"	90	25	−805	−782	1.4×10^{-6}	−204	54
*15	"	90	25	−813	−806	9.0×10^{-7}	−162	61
*16	"	90	80	−844	−829	2.0×10^{-6}	−170	49

* Electrolyte pre-saturated with hydrogen.

Table 7. Corrosion rates of plain and welded carbon steel coupons exposed to granitic groundwater at 90°C with hydrogen gas overpressures of 1, 10 and 100 atmospheres

Hydrogen Overpressure Condition Exposure (days)	1 Atmosphere Plain	Weld	10 Atmospheres Plain	Weld	100 Atmospheres Plain	Weld
	(Average corrosion rates in μm/year)					
120	0.47	0.08	1.09	0.93	0.92	0.47
243	0.22	*	0.58	0.58	0.50	0.78
389	*	*	0.74	0.50	0.38	0.20
552	0.16	0.10	0.82	0.59	0.49	0.31
999	0.18	0.13	0.63	0.39	0.37	0.21
1481	0.15	0.15	1.49	0.63	0.25	0.20

* These coupons exhibited slight weight gains which were within the experimental error.


Gas evolution measurements

The results of the gas generation experiments are expressed as (i) corrosion rate in μm yr-1, calculated assuming Fe_3O_4 was the corrosion product, and (ii) the volume of gas produced in dm^3 H_2 m^{-2} yr^{-1}. The volumes of gas produced were normalised to standard temperature (273K, 0°C) and pressure (760 mm Hg). The 'instantaneous' corrosion rates, determined from the volume of gas evolved between regular readings divided by the elapsed time between readings, are presented graphically as a function of exposure period for various test environments. Control cells, that contained no carbon steel, gave background changes of <0.2 dm^3 m^{-2} $year^{-1}$ at 50°C. In the next sections, the effects of the various environmental variables on the anaerobic corrosion rates of carbon steel are summarised.
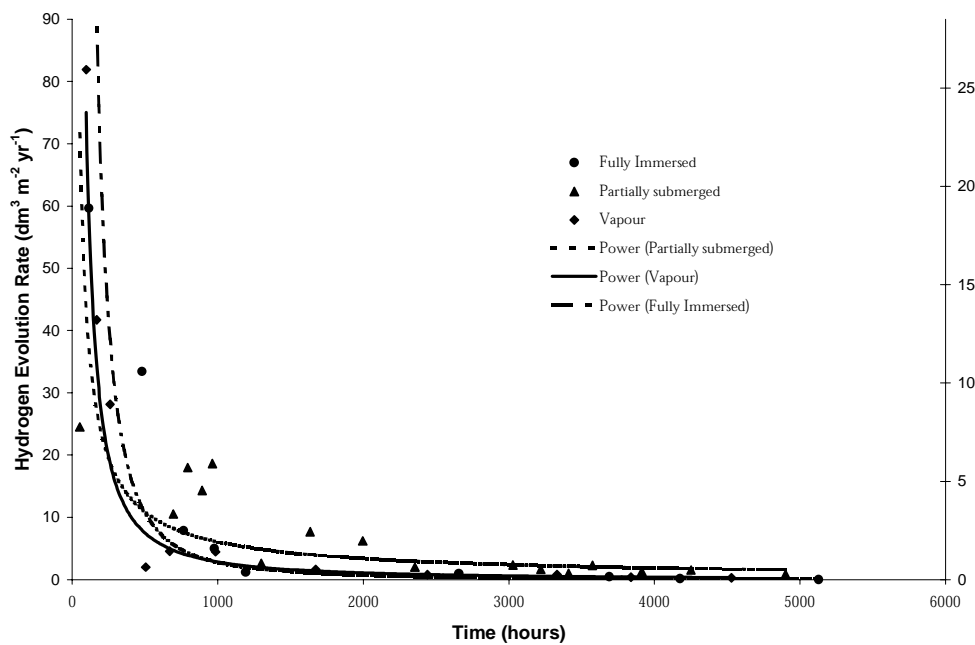

KBS TR 36 groundwater

The results of the hydrogen evolution tests in KBS TR 36 groundwater at 30°C and 50°C are presented in Figure 12. Samples that were pickled showed higher initial rates than samples that were only degreased. The corrosion rate declined with increasing exposure time, with >95% decline occurring during the first 1500 hours. The corrosion rate was higher at 50°C than at 30°C. These results were used as a baseline measurement to be compared with other test environments. In subsequent experiments the specimens were always used in the pickled condition unless otherwise stated.

Degree of immersion

The effect of the degree of immersion on the gas generation rate is shown in Figure 13. Differences were observed in the initial hydrogen production rates and the rate of decline as a protective corrosion product layer developed. The hydrogen production rate for partially-submerged carbon steel wires was initially less than for totally submerged wires or wires which were clear of the groundwater. The partially-submerged wires also exhibited a slower rate of decline in hydrogen production rate, even though a black magnetite film was clearly visible over most of the surface. The total amount of hydrogen produced by the partially immersed wires after 5000 hours was about 10% larger than from the fully immersed wires, suggesting that the final thicknesses of the protective magnetite layers were similar.
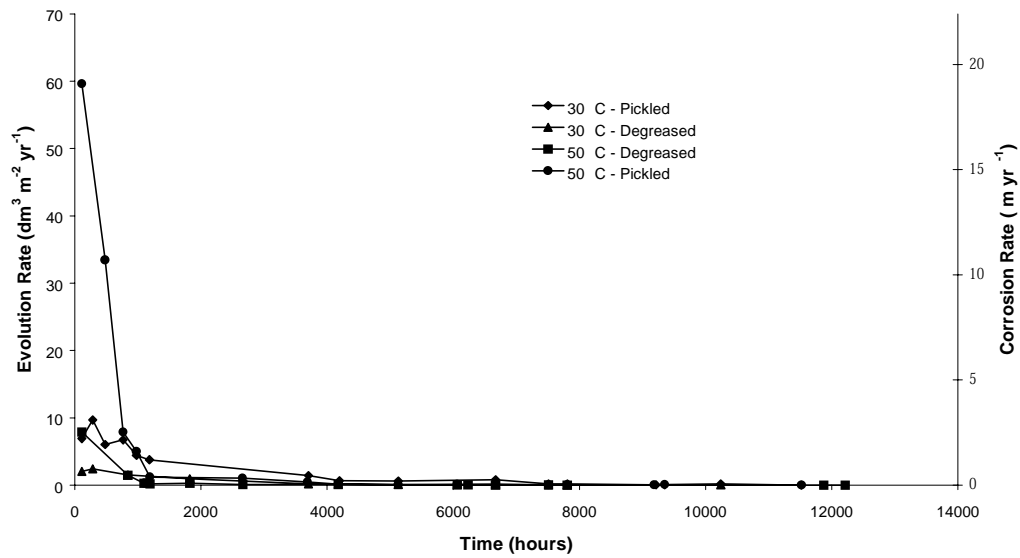
Figure 12. *Rate of evolution of hydrogen produced by anaerobic corrosion of carbon steel in anoxic artificial KBS TR 36 groundwater, at 30°C and 50°C, showing effect of pickling and degreasing before experiment.*
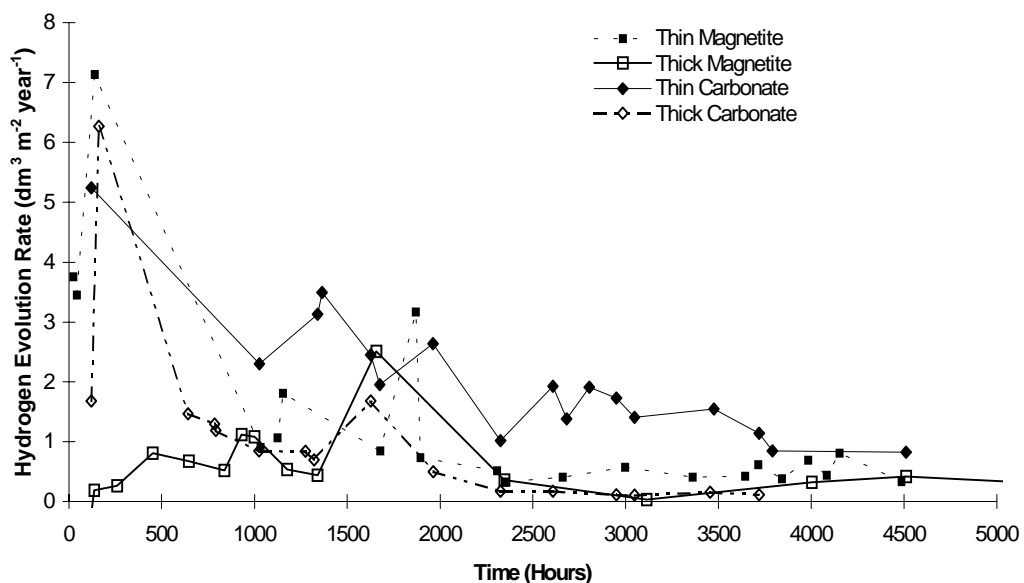

Figure 13. *Rate of evolution of hydrogen produced by anaerobic corrosion of pickled carbon steel at 50°C, showing the effect of the degree of immersion in anoxic artificial KBS TR 36 groundwater.*

Effect of pre-formed film composition

The effect of magnetite and carbonate films on the rate of gas production is shown in Figure 14. Both types of film were able to reduce the initial burst in the hydrogen production rate that is observed on pickled metal surfaces, with the order of increasing effectiveness being: thin carbonate < thin magnetite < thick carbonate < thick magnetite. The thick magnetite film specimens showed very little corrosion, with an apparent negative rate of hydrogen production during the first 100 hours. At all times the rates were below those measured on unfilmed (i.e. pickled) specimens at comparable times.

Effect of ferrous ion

The effect of increasing the concentration of ferrous ions, sulphate ions and carbonate ions is shown in Figure 15. The presence of 0.1M $FeSO_4$ resulted in significantly increased long-term corrosion rates, compared to normal KBS TR 36 groundwater. Additionally, there appeared to be very little formation of the expected magnetite film, but a black precipitate was observed on the bottom of the cell. This may have been because a non-protective layer of $FeSO_4$ may have formed on the surface of the wires and prevented adherence of protective magnetite. Alternatively, iron sulphate may have caused iron carbonate to precipitate out of solution, thus leading to a decrease in the pH and formation of a more aggressive environment. At the end of the experiment the test solution was pH 7.3, compared to pH 8.1 of freshly prepared KBS TR 36 groundwater. A freshly prepared solution of 0.1M $FeSO_4$ in KBS TR 36 groundwater had an initial pH of 6.5. It therefore appears that the increase in corrosion rate observed in these experiments was largely due to a shift in the pH towards more aggressive conditions. However, a control cell, which contained 0.1M K_2SO_4 instead of iron sulphate, also showed a larger than expected long-term corrosion rate, although almost an order of magnitude less than that with the $FeSO_4$. The pH of this control solution was found to be pH 8.9 at the end of the experiment, therefore it would appear that sulphate can cause an increase in the long-term corrosion rate without the need for a shift in the pH. An alternative explanation for the long-term increase in hydrogen production with sulphate may be that it simply increased the ionic strength of the groundwater, an issue that is discussed in more detail below.

Figure 14. *Rate of evolution of hydrogen produced by anaerobic corrosion of pickled carbon steel at 50°C, showing the effect of pre-coating with either a magnetite or iron carbonate layer, with approximate thicknesses of 50 nm or 500 nm.*
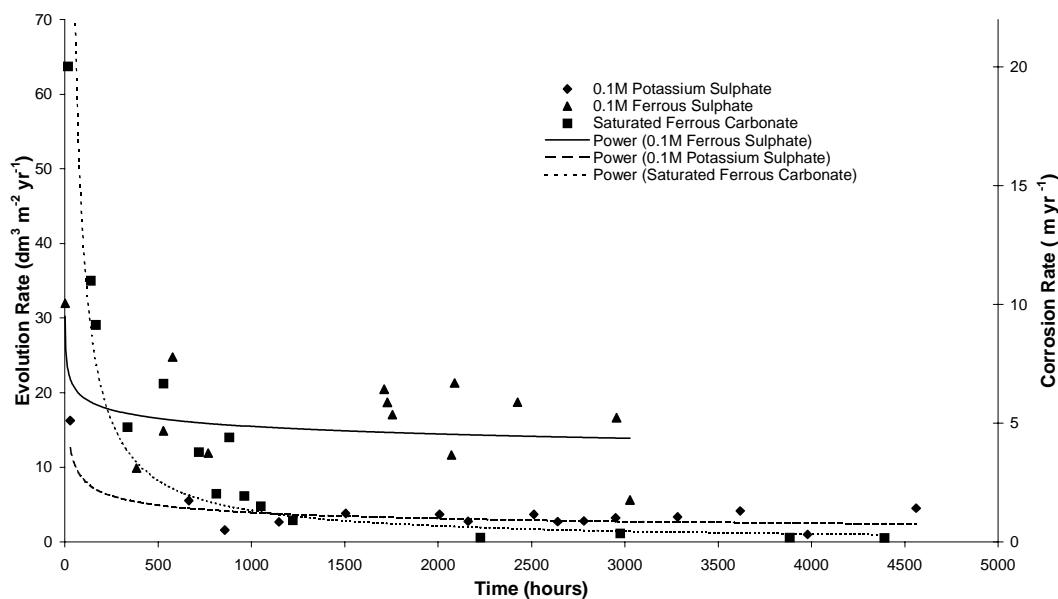
Figure 15. *Rate of evolution of hydrogen produced by anaerobic corrosion of pickled carbon steel in anoxic artificial KBS TR 36 groundwater at 50°C, showing the effect of adding 0.1M FeSO₄ or 0.1M K₂SO₄, or saturating with FeCO₃.*

To overcome the problem of salt precipitation and the accompanying pH shifts, the experiment was repeated using KBS TR 36 groundwater saturated with $FeCO_3$. The low solubility constant of $FeCO_3$ meant that Fe^{2+} saturation was achieved without the precipitation of any of the components of the standard granitic groundwater (Table 2), so that the pH was not disturbed. Carbonate is likely to be the dominant anion in the repository, so this experiment represented a more realistic Fe^{2+} concentration than the experiment with iron sulphate. The rates of hydrogen production and corrosion were similar to those observed in the absence of the $FeCO_3$, suggesting that the concentration of Fe^{2+} ions in the repository groundwater did not significantly affect the rate at which protective magnetite films are formed.

Effect of radiolysis products

The addition of 9 mM NH_3 or 3 mM HNO_3 to KBS TR36 groundwater at 50°C had a minor effect on the hydrogen evolution rate (Figure 16). In both cases, the additions reduced the initial corrosion rate, resulting in a lower total volume of hydrogen than in normal artificial KBS TR 36 groundwater. The long-term hydrogen evolution rates were unaffected by either the ammonia or nitric acid additions.

Effect of ionic strength

The effect of a 10-fold increase in the ionic strength of the KBS TR36 groundwater on the corrosion rate of carbon steel wires is shown in Figure 16. Increasing the ionic strength caused a decrease in the hydrogen production rates observed during the first 500 hours compared to more dilute groundwater. However, the corrosion rate after the protective magnetite film had formed (>1000 hours) was approximately an order of magnitude greater than in dilute groundwater.
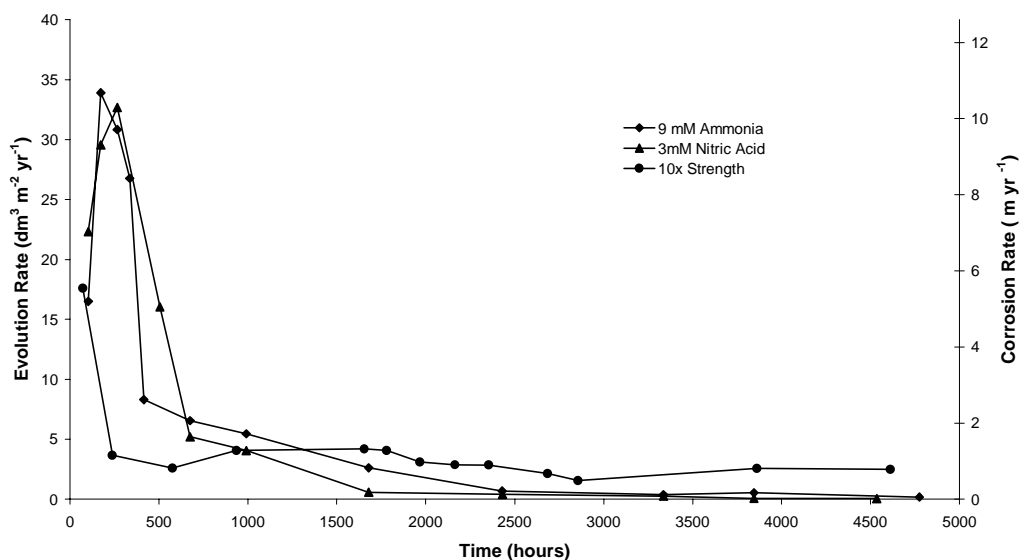
Figure 16. *Rate of evolution of hydrogen produced by anaerobic corrosion of pickled carbon steel in anoxic artificial KBS TR 36 groundwater at 50°C, showing the effect of adding 9 mM NH₃ or 3 mM HNO₃, to simulate the products of radiolysis reactions involving nitrogen and water, and the effect of increasing the ionic strength by 10× the strength of the standard composition.*

Effect of groundwater composition

Figure 17 shows the hydrogen evolution rate for carbon steel in Äspö groundwater and Bentonite-equilibrated groundwater. The initial hydrogen evolution rates in Äspö water were similar to other high ionic strength groundwaters at the same pH (e.g. the 10´ strength KBS TR 36 groundwater), but the long-term hydrogen evolution rates were at least five times higher in high ionic strength groundwater than in dilute groundwaters. The gas generation rate in bentonite-equilibrated water was depressed compared to other groundwaters of similar ionic strength. The addition of 0.1M Na_2SO_4 to bentonite-equilibrated groundwater had no significant effect on the hydrogen evolution rate. The pH of both groundwaters fell from pH 10.5 to pH 9.8 during the 5,000 hours of the test.

Comparison of cast iron with carbon steel

The hydrogen evolution rates and corrosion rates for carbon steel and cast iron in artificial Äspö groundwater and groundwater equilibrated with bentonite at 50°C are presented in Figure 18. In Äspö water the initial anaerobic corrosion rates were similar for cast iron and carbon steel. However, the hydrogen evolution rates fell rapidly during the first 500 hours, with the rate of decrease being slightly greater for the cast iron than the carbon steel. After 1000 hours the hydrogen evolution rates from the cast iron were approximately three times lower than those observed for carbon steel after a similar time period. After 5,000 hours the corrosion rate was approximately five times lower for the cast iron (0.1 μm yr⁻¹ for cast iron compared to 0.5 μm yr⁻¹ for carbon steel).

In bentonite-equilibrated water the initial hydrogen evolution rates were approximately the same for cast iron and carbon steel. The rates were approximately four times less than in Äspö groundwater. The gas generation rates decreased rapidly over the first 1,000 hours or so, but the cast iron corrosion rate decreased more quickly. The corrosion rate after 5,000 hours was approximately five times lower for the cast iron than the carbon steel (0.01 μm yr⁻¹ for cast iron compared to 0.05 μm yr⁻¹ for carbon steel).

31
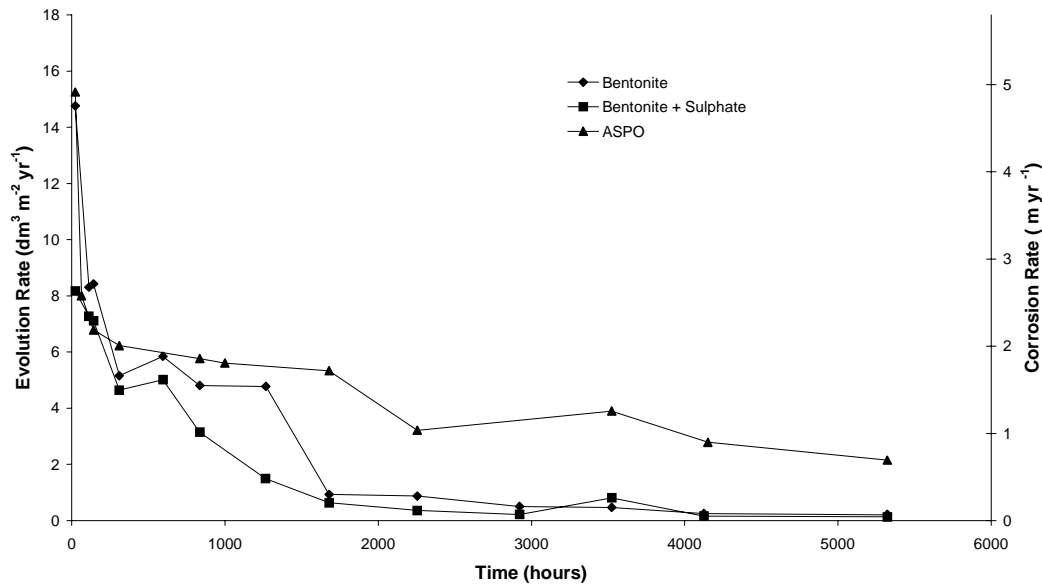
Figure 17. *Rate of evolution of hydrogen produced by anaerobic corrosion of pickled carbon steel in anoxic artificial groundwaters.*
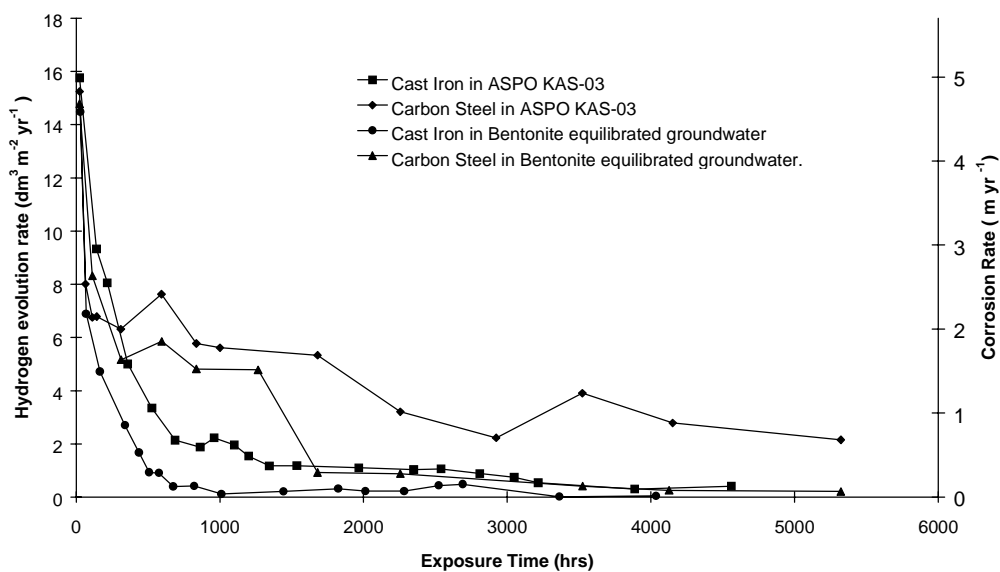
Figure 18. *Hydrogen evolution rates and anaerobic corrosion rates for cast iron and carbon steel in artificial Äspö groundwater and groundwater equilibrated with bentonite at 50 °C.*

At the end of the experiments, the specimens appeared dark grey. Some dark grey friable corrosion product was also observed floating on the surface of the test solution and lying at the bottom of the cell.

Figure 19 shows the hydrogen evolution rates and the equivalent corrosion rates for carbon steel and cast iron in Äspö water at 85°C. A comparison of this figure with the data for 50 °C shows that the increase in temperature caused the initial hydrogen evolution rate to increase by approximately an order of magnitude. However, the cast iron and
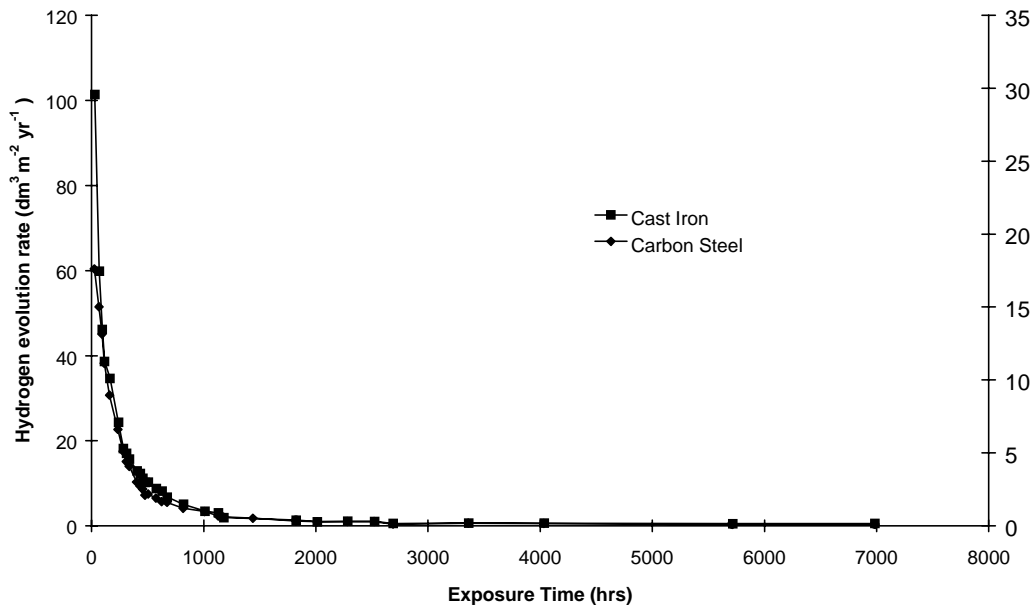
Figure 19. *Hydrogen evolution rates and anaerobic corrosion rates for cast iron and carbon steel in artificial Äspö groundwater, at 85 °C.*

carbon steel behaved almost identically, in contrast to the behaviour at 50°C where the carbon steel exhibited higher corrosion rates. The corrosion rate after 5,000 hours was approximately 0.1 μm yr^{-1} for both metals, which is approximately the same as the value at 50 °C in untreated groundwater but about ten times higher than in bentonite-equilibrated groundwater at 50 °C.

Effect of removing adherent corrosion product

Prior to removal of the outer magnetite layer, the rate of hydrogen evolution on the carbon steel had been approximately 0.2 dm^3(STP) m^{-2} year^{-1}. After the outer magnetite layer had been removed there was only a minor increase in the hydrogen evolution rate once the steel had been re-immersed in artificial groundwater. The maximum hydrogen evolution rate observed was at least two orders of magnitude slower than that observed on pickled carbon steel wires. Within approximately 100 hours the hydrogen production rate was virtually the same as it had been prior to the mechanical disruption to the magnetite film caused by the tissue paper, and complete recovery was achieved after about 1500 hours.

Discussion

Electrochemical measurements – atmospheric pressure

Open circuit potential

The equilibrium water reduction potential at pH 8.1 is approximately –720 mV at 25°C and –760 mV at 50°C. The rest potentials of both the pickled and unpickled specimens were more negative than the hydrogen reduction potential, by 25 to 55 mV, indicating a potential to generate hydrogen by water reduction, at both temperatures. As the corrosion product film thickened the potential became more positive. A positive shift in open-circuit potential would cause an increase in the corrosion rate of cathodically-limited corrosion, but either a decrease or no change in the corrosion rate of an anodically-limited reaction. The positive shift in the open-circuit potential of the carbon steel which occurred as the corrosion product film developed, corresponds to a time during which the hydrogen evolution rate on carbon steel was observed to decrease in gas generation experiments. These observations are consistent with the corrosion process becoming anodically-limited by the corrosion product film.

Tafel slopes

The corrosion rates calculated from the Tafel slope measurements for a pickled sample (~23 μm/yr) and a magnetitite-coated sample are in good agreement with the rates calculated from gas evolution measurements during the first 100 hours, but much higher than the long-term gas evolution measurements. It is likely that the 74.1 mV dec^{-1} Tafel slope observed with the magnetite-covered specimen was due to the dissolution of Fe^{2+} ions, but with the process being inhibited by the transport of the cations through the magnetite film.

At potentials more positive than –450 mV vs SCE the value of the Tafel slope of the magnetite covered carbon steel specimen began to decrease further, indicating that the passivity of the magnetite film was increasing. One possible explanation for this behaviour is the production of hematite:

$$2Fe_3O_4 + H_2O \rightarrow 3Fe_2O_3 + 2H^+ + 2e^- \tag{5}$$

the standard potential for which is –0.462 V vs SCE at pH 7.5. There are a number of alternative Fe(III) compounds which could also have resulted in passivity. Figure 5 shows that the overall effect of the magnetite film was to reduce the rate of the anodic reaction, i.e. the corrosion reaction was anodically-limited, in agreement with the conclusions from the corrosion potential measurements.

The Tafel slope measurements obtained using the film-free static and rotating disc electrodes (60 mV dec^{-1}) were in reasonable agreement with the values of other workers (typically between 30 mV dec^{-1} and 100 mV dec^{-1}).

The value for the cathodic Tafel slopes were in the region of 50 mV dec^{-1} (Table 4). This value is significantly below the value of approximately 120 mV dec^{-1} expected for the reaction scheme:

$$H_2O + e^- \Rightarrow H_{ads} + OH^- \tag{8}$$

$$2H_{ads} \Rightarrow H_2 \tag{9}$$

in which the rate controlling step is step (8). This is thought to be the mechanism for hydrogen evolution on iron in acid solutions. The lower value found in the present work is more consistent with the following reaction scheme:

$$H_2O + e^- \Rightarrow H_{ads} + OH^- \tag{10}$$

$$H_{ads} + H_2O + e^- \Rightarrow H_2 + OH^- \tag{11}$$

which gives a cathodic slope of 40 mV dec^{-1} when the reaction is limited by the surface coverage of H_{ads}. The corrosion current, that can be obtained from this data by extrapolation of the Tafel lines, has a value of approximately 10^{-7} A/cm^2 which, assuming the corrosion process is forming ferrous hydroxide, corresponds to a corrosion rate of approximately 1 μm year^{-1}. This is in reasonable agreement with the corrosion rates obtained by other workers[6,7] in relatively short term tests of less than 100 days duration.

ZRA measurements

It is proposed that the corrosion product film consists of an inner oxide overlaid by a porous ferrous hydroxide / ferrous carbonate layer and that the outer portion of this porous layer exhibits increased levels of transformation to magnetite as the temperature increases above 50°C. On this basis three rate controlling steps can be considered:

i. Control of the cathodic reaction by hydrogen concentration at the metal/oxide interface and hence by diffusion of hydrogen through the porous oxide layer;

ii. If the phase oxide were continuous, the hydrogen evolution reaction would occur on the outside of the oxide rather than on the metal and hence the hydrogen overpotential would be rate limiting;

iii. Control of the anodic reaction by the concentration of ferrous ion.

The ZRA measurements using galvanically coupled platinum and carbon steel electrodes were carried out to investigate the rate controlling step in the anaerobic corrosion process.

Mechanism (i). If hydrogen diffusion through the oxide were rate controlling, and the structure of the oxide were as described above, the effect would be for the hydrogen evolution reaction to transfer to the platinum of a platinum-steel couple. As the corrosion process proceeded, and the corrosion film thickened, hydrogen evolution on the carbon steel would be less favoured so more of the hydrogen evolution reaction should transfer to the platinum. Therefore the galvanic current flowing through a zero resistance ammeter (ZRA) connected between the two metals should increase with time. If the porous oxide structure were duplex with a magnetite outer layer, as suggested for temperatures above 50°C, the thicker film would result in magnetite depositing within the pores, eventually blocking them. In the extreme this would produce a barrier oxide. Although the initial response recorded on a ZRA may be the same as that below 50°C, with film formation causing increased transfer of the hydrogen evolution reaction to the platinum, the galvanic current flow between the two electrodes would eventually decay as the oxide compacted.

Mechanism (ii). If the hydrogen over-potential were rate controlling, with the reaction occurring on the inner oxide, the couple current measured on the ZRA would be the same for both temperature ranges, at least until the outer layer thickened sufficiently to make hydrogen diffusion rate limiting.

Mechanism (iii). If the anodic reaction were rate limiting similar behaviour should be observed in both temperature regimes, since the concentration of ferrous ions and hence the electrode potential, would remain constant. Therefore the couple current should be constant, or decrease if hydrogen evolution became rate controlling.

The steady currents found in three of the four experiments conducted at 25°C are therefore not consistent with hydrogen diffusion through a porous layer being the rate controlling step. Instead, the steady currents are more consistent with ferrous ion control (mechanism (iii) above).

Scratching electrode

If an iron or steel electrode is placed into a solution at pH above 8.0, it naturally forms a passivating oxide layer. It is well known that if this oxide layer becomes damaged, it will rapidly reform as long as dissolved oxygen is present in the solution. However, whether such a repassivation process can occur in the absence of oxygen depends on the balance between the peak repassivation current and the current available from the water reduction reaction. If no passive film forms, the electrode will undergo active dissolution. Whether the carbon steel electrode is active or passive, an oxidising current will be required. Under open-circuit conditions such a current can only be supplied by the reduction of a solution species, and in the case of a clean aqueous system, oxygen and water are the only two oxidants available. The scratching electrode experiments in aerated conditions show that repassivation occurred rapidly in the presence of oxygen.

At very low levels of dissolved oxygen, the required oxidising current must come from the water reduction reaction. This can only occur if the rest potential of the iron or steel specimen is below the hydrogen evolution potential (-0.712 V vs SCE at pH 8.0). At such low potentials the existence of a stable Fe_3O_4 film is possible /Pourbaix et al 1974/. The rapid repassivation following the scratching experiment in deaerated conditions (Figure 10a) could be because the cathodic process required for the repassivation of the scratch in the absence of oxygen was partial reduction of the remaining Fe_2O_3 film on the unscratched part of the electrode surface:

$$2Fe + 3H_2O \Rightarrow Fe_2O_3 + 6H^+ + 6e^- \tag{12}$$

$$3Fe_2O_3 + 9H_2O + 6e^- \Rightarrow 6Fe^{2+} + 18\ OH^- \tag{13}$$

This mechanism is consistent with observations from rotating ring disc electrode experiments /Sykes et al 1986/ and suggests that Fe_2O_3 is a good oxidising agent and that its apparent passivity is predominantly due to the lack of readily available oxidisable species.

After the second scratch (Figure 10b), when repassivation did not appear to occur, it appears that insufficient oxide remained on the electrode surface to regenerate a complete Fe_2O_3 layer over the scratch. The new open-circuit potential was within a few millivolts of the hydrogen evolution potential, indicating that only a very small over-potential was required for the water reduction reaction to balance the new anodic process occurring on the carbon steel electrode. This in turn means that the corrosion process must have been slow. There was no evidence of any corrosion product on the electrode surface, indicating that the anaerobic active dissolution process is probably slower than its aerobic counterpart.

In the absence of bicarbonate (Figure 11), the recovery time was much longer than in its presence, indicating a marginally passivating film on the electrode surface, probably due to Fe_3O_4. However, as the final rest potential was approximately ten millivolts below the hydrogen evolution potential, active dissolution was almost certainly still occurring across this film.

Effect of hydrogen overpressure

Corrosion reactions that are cathodically limited by the rate of hydrogen evolution should exhibit a correlation between their corrosion potentials and the applied hydrogen overpressure. This correlation is usually a negative shift in the corrosion potential of 60 mV for every decade increase in hydrogen overpressure /Pourbaix et al 1974/, resulting from a corresponding shift in the equilibrium potential of the hydrogen reduction reaction. No correlation between either the rest potential with hydrogen overpressure was observed, indicating that the anaerobic corrosion of carbon steel in 3.5% NaCl is not cathodically limited. As expected the electrochemically derived corrosion rate, expressed as a current density, i_{corr}, was much greater than that estimated from the weight loss coupons in long term immersion tests.

From the data in Table 7 it appears that slightly higher corrosion rates occurred at elevated hydrogen overpressures. This is an unexpected result, as equation (2) predicts a decrease in corrosion rate with increasing hydrogen overpressure. However, the results were within the experimental uncertainties, and it can be concluded that the anaerobic corrosion rates were independent of hydrogen overpressure.

Corrosion product

Reference to the Pourbaix diagram shows that for iron held close to the hydrogen evolution potential in a solution of around pH 8.0 both the formation of an Fe_3O_4 film and active dissolution to Fe^{2+} ions are thermodynamically feasible. As active dissolution proceeds both the concentration of Fe^{2+} ions and the pH of the solution should increase, making corrosion less thermodynamically favourable, and the corrosion rate should fall with time.

Hydrogen evolution

In all tests the corrosion rate decreased with increasing exposure time, as the film of corrosion product thickened. This suggests that the protective films did not crack as they thickened, since such behaviour would have resulted in bursts of hydrogen production. The hydrogen evolution process on carbon steel in anaerobic groundwaters can be divided in two regions, namely short-term and long-term. In the short-term (<1500 hours), the hydrogen evolution rates were initially high, but then rapidly declined. In the long-term the hydrogen evolution rate was virtually constant. This behaviour is similar to that reported by Kreis /Kreis 1991; Kreis et al 1992/, Simpson /Simpson et al 1988; Simpson et al 1985; Schenk 1988/ and Grauer /Grauer et al 1991; Grauer 1988/ who showed that the corrosion rate in anaerobic, neutral or alkaline conditions falls with time over a period of several thousand hours.

The literature relating to the corrosion of iron at low potentials contains strong evidence that Fe(OH)$_2$ and Fe$_3$O$_4$ surface films thicken until their rate of growth is balanced by their rate of dissolution at the oxide/electrolyte interface /Davies et al 1980; Bignold et al 1981/. In such circumstances, the rate of metal dissolution is determined by the rate of diffusion of metal ions from the metal interface. The published work implies that the films grow by a 'high field' process driven by the potential gradient across the film in the case of Fe(OH)$_2$, and by diffusion in the case of the electrically conducting Fe$_3$O$_4$. Both of these processes predict that, in the absence of dissolution, film thickening will decrease with time to a negligible rate long before the film has thickened to the point at which spallation might occur.

Degree of immersion

Differences were observed in the initial gas generation rate between specimens that were fully immersed, partially immersed and exposed to water vapour only, but the long-term rates were very similar. Vapour that condensed out on the carbon steel would have had a lower pH than the bulk groundwater, as the buffering salts would not have existed in the vapour phase. A lower pH would be expected to produce a higher corrosion rate, as was observed in the early stages of the experiments. However, the faster corrosion rate would have led to a more rapid build-up of protective corrosion product, and caused a more rapid decline in corrosion rate. Furthermore, in water vapour it would not have been possible for soluble Fe^{2+} ions to diffuse away from the surface into bulk solution, hence the surface concentration of ferrous ions would have been higher.

On the partially immersed specimens, there would have been a pH gradient between the condensed water vapour and the test solution. This could have resulted in a form of galvanic coupling, with increased hydrogen production in the low pH water vapour regions and increased magnetite formation in the high pH submerged regions. The magnetite might be expected to spread slowly up the wires, from the submerged ends, giving rise to the observed gradual decrease in the hydrogen production rate.

Effect of pre-formed film composition

The low corrosion rates measured for material with pre-formed surface films indicate that the development of corrosion product film caused the decrease in the corrosion rate that was observed during the first 1500 hours with pickled carbon steel samples. The final equilibrium corrosion rates for all the pre-coated specimens were similar to the pickled samples, although the thin carbonate film did result in a slightly higher value. This suggests that magnetite was more protective than carbonate.

Effect of ferrous ion

The concentration of ferrous ions in solution did not significantly affect the rate of hydrogen production. One explanation for this is as follows. The corrosion product is believed to consist of two layers of magnetite, namely an inner and an outer layer. The outer layer is formed by precipitation, and therefore its rate of growth would be expected to depend on the ferrous ion concentration. However, the majority of the corrosion protection is believed to be provided by the inner film, which forms directly on the surface of the steel by an electrochemical mechanism without going through a ferrous ion intermediate stage. Consequently its development is less likely to be affected by the ferrous ion concentration.

Effect of radiolysis products

The reduction in the initial corrosion rate of the carbon steel in the presence of ammonia can be explained by the increase in pH that the addition would have caused. However, the addition of 3 mM HNO_3 should have caused the pH to fall considerably, perhaps down to pH 3, and therefore would be expected to increase the corrosion rate. One possible explanation is that the experimental technique was not able to monitor the hydrogen that was evolved in the first 48 hours after the carbon steel was placed in the groundwater. If the corrosion rate was very high during this period the nitric acid may have been completely consumed before any readings could be taken. The lack of any long-term influence of nitric acid on the corrosion rate of the carbon steel may be due to the increased solubility of Fe^{2+} at lower pH values. This would have resulted in the bulk pH of the groundwater rising as the nitric acid corroded the carbon steel by the following reaction:

$$Fe + 2H^+ \rightarrow Fe^{2+} + H_2\uparrow \qquad (14)$$

As the protons were consumed, and the pH rose, the cathodic reaction would have reverted to the reduction of water, which is the dominant reaction for the corrosion of iron in anaerobic conditions. Calculations show that the nitric acid added to the test solution would have been consumed with the first day or two of the test. The cathodic reduction of NO_3^- to NO_2^- could also have occurred in competition with the hydrogen evolution reaction although the low concentration of nitrate means that it is unlikely to have had any significant long-term effect.

Effect of ionic strength

The long-term hydrogen evolution rate was at least five times faster in high ionic strength groundwater than in the dilute groundwaters, but there was no initial burst of corrosion in the high ionic strength water, whereas there was in dilute groundwaters. This suggests that the time required to form a thick protective magnetite film was longer in more concentrated solutions. This view is supported by the observation that the black film did not appear to be as coherent in concentrated solutions as in dilute solutions. Possible explanations for the higher hydrogen evolution rates in high ionic strength solutions are:

1. Increased competition between the formation of magnetite and other less protective iron salts, such as $FeCO_3$ or $FeSO_4$;

2. Increased availability of anions to form more soluble corrosion products, for example $FeCl_2$ instead of $Fe(OH)_2$, and hence reduced ability to form a protective magnetite film;

3. Incorporation of ions in the magnetite film increasing its conductivity, and possibly increasing its effectiveness as a hydrogen electrode;

4. Local buffering of the pH; magnetite is more thermodynamically favoured at high pHs, therefore the protective hard inner film may only form when the pH at the carbon steel / groundwater interface is significantly higher than the pH of the bulk solution.

5. A decrease in the thickness of the protective hard inner magnetite layer due to local buffering of the pH. The water reduction reaction will lead to an increase in the pH at the carbon steel/groundwater interface, to a value that will be limited by the buffering capacity of the groundwater. Since the formation of magnetite is more thermodynamically favoured at high pHs, its thickness could decrease as the buffering capacity of the groundwater increases. The buffering capacity of a groundwater is likely to increase with its ionic strength.

6. Increased conductivity may enable more efficient electron transfer to occur between the carbon steel and the water that is reduced to hydrogen, leading to a higher corrosion rate.

The visual observation that the black magnetite films formed tended to be less coherent in the more concentrated groundwaters tends to support explanation 1.

The ionic strength of groundwater containing 0.1M K_2SO_4 was approximately three times that of the 10-fold ionic strength groundwater, yet the two solutions yielded virtually identical hydrogen evolution rates. This suggests that the dependence of the hydrogen evolution rate on ionic strength is restricted to a domain below a threshold value, which lies somewhere between that of the standard and 10-fold strength groundwaters. Above this limit, further increases in the ionic strength of the groundwater are not expected to affect the hydrogen evolution process. The similarity between the results from the 0.1M K_2SO_4 and the 10-fold strength groundwaters supports the idea of increased electron transfer efficiency in the more conductive solutions. Once sufficient conductivity has been reached it is likely that the particular electron transfer process involved is no longer the rate limiting step.

Effect of groundwater composition

The lower rate of hydrogen production on carbon steel in the bentonite-equilibrated groundwater compared to other groundwaters is probably due to its higher pH, which was 10.5, compared to 8 for the Äspö groundwater. The higher pH favours the formation of magnetite over active dissolution and decreases the solubility of Fe^{2+} ions, leading to more rapid formation of a protective magnetite film. This supports the suggestion that the influence of the ionic strength on the corrosion rate of the carbon steel is due to changes in the buffering capacity at the carbon steel/solution interface. The long-term hydrogen production rate (> 5000 hours) on carbon steel in bentonite-equilibrated groundwater was slightly less than that found in dilute groundwaters, but the difference was within the error limits of the experimental arrangement.

It can be concluded that although high ionic strength groundwaters increase the rate of hydrogen production on carbon steel, the increase can be offset by increasing the pH. The addition of 0.1M Na_2SO_4, to bentonite-equilibrated groundwater had no experimentally significant effect on the hydrogen evolution rate.

Effect of temperature

The large increase in the initial corrosion rate with increasing temperature is indicative of an activation-controlled process, which would be expected to follow an Arrhenius relationship /Boden 1994/. As the film develops, the corrosion rate becomes determined by the diffusion of various species through the oxide film, a process which is considerably less sensitive to increasing temperature. The composition of the corrosion product would be expected to change form ferrous hydroxide at temperatures below 50°C to magnetite at higher temperatures /Linnenbom 1958/, although the composition was not determined in this work.

Comparison of cast iron with carbon steel

The long-term anaerobic corrosion rate for cast iron in granitic groundwaters at 50°C was approximately five times lower than observed with carbon steel. It was lowest in the bentonite-equilibrated groundwater. The differences in corrosion rate between the two materials suggest that there must have been subtle differences in the rate controlling steps involved in the corrosion mechanism. At temperatures above 50°C it is possible that the oxide produced in anaerobic conditions grows by outward diffusion of ferrous ions from the metal-oxide interface, which could be affected by small changes in the structure of the oxide film caused by the different composition and microstructure of the substrate. An alternative explanation may be that the oxide film is more adherent to cast iron than to carbon steel; similar behaviour has been observed in seawater where cast iron corrodes two to four times more slowly than carbon steel /Kreysa et al 1992/.

Increasing the temperature from 50 °C to 85 °C caused the short-term (<500 hours) hydrogen evolution rate for both carbon steel and cast iron to increase by an order of magnitude, but in the long-term the corrosion rates were similar to that for cast iron at 50°C.
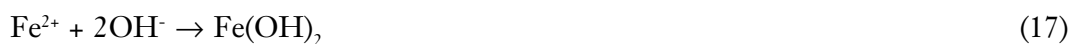
Effect of removing adherent corrosion product

The gas generation rate did not increase significantly after removal of the non-adherent corrosion product, suggesting that the majority of the protection afforded by the magnetite film was provided by a hard inner layer. This layer was not significantly damaged by either the removal of the outer magnetite layer with tissue paper, or any mechanical damage arising when the carbon steel was transferred from one reaction vessel to another. It can therefore be concluded that minor mechanical disturbance to the magnetite film on the inner carbon steel container is unlikely to result in large bursts of hydrogen production.

The strongly adhering inner part of the dual layer structure of the magnetite films probably formed directly on the carbon steel by the electrochemical reaction;

$$3Fe + 4H_2O \rightarrow Fe_3O_4 + 4H_2 \tag{15}$$

The easily removable layer is likely to have been formed by a precipitation process, such as;

$$Fe + 2H_2O \rightarrow Fe^{2+} + H_2 + 2OH^- \tag{16}$$

$$Fe^{2+} + 2OH^- \rightarrow Fe(OH)_2 \tag{17}$$

$$3Fe^{2+} + 4H_2O \rightarrow Fe_3O_4 + 8H^+ + 2e^- \tag{18}$$

A similar explanation has been proposed for the dual layer magnetite structure found on boiler tubes /Shoesmith et al 1981/.

Conclusions

The main conclusions from this paper are as follows:

1. Carbon steel undergoes active anaerobic corrosion in artificial Swedish granitic groundwater, although a magnetite film retards the rate of corrosion. The outer layer is a loose porous film that is easily disrupted, while the inner layer is adherent and crystalline and forms the main rate-controlling layer.

2. The anaerobic corrosion rate of bare carbon steel at 30°C, 50°C and 85°C is of the order of 10 to 30 μm year^{-1} initially, but as an oxide film forms the rate decreases to <0.1 μm year^{-1}. The initial corrosion rate increases with increasing temperature.

3. Hydrogen overpressures up to 100 atmospheres have no significant effect on the corrosion rate or the corrosion potential. This suggests that the corrosion reaction is therefore anodically limited, rather than cathodically limited.

4. Higher anaerobic corrosion rates occur above an ionic strength threshold.

5. The anaerobic corrosion rate is not limited by the concentration of dissolved ferrous ion.

6. The presence of the radiolysis products ammonia and nitric acid do not significantly affect the anaerobic corrosion rate.

7. No localised corrosion initiates under anoxic conditions.

8. Welding has no effect on the anaerobic corrosion rate in granitic groundwaters.

9. The long-term anaerobic corrosion rate of cast iron is approximately five times lower than for carbon steel in the same solution, at 50°C.

10. The long-term anaerobic corrosion rates of both cast iron and carbon steel are lower in groundwaters at higher pH, due to a more stable oxide film.

11. In both aerated and deaerated conditions, physical damage to the surface has only a short transient effect on the corrosion rate. The rate of film reformation does not depend on the presence of dissolved oxygen, because the oxygen required to form the film is provided by direct reaction between bare steel and the water. If a passive Fe_2O_3 film exists before anoxic conditions develop, the film can undergo a reduction process to provide the current required to regenerate a magnetite film.

Acknowledgements

References

Bignold G J, de Whalley C H, Garbett K, Garnsey R, Woolsey I S, Libaert D F and Sale R, "Erosion Corrosion of Mild Steel in Ammoniated Water", Proc 8th Int. Congress on Metallic Corrosion, 1981.

Bockris J O'M, Genshaw M A, Brusic V, Wroblowa H, Electrochim. Acta 16, (1971): p. 1859.

Boden P J, Effect of Concentration, Velocity and Temperature, Chapter 2.1 in Corrosion, (Butterworth Heinemann, 1994).

Brookins D G, Eh-pH Diagrams for Geochemistry(Berlin New York: Springer-Verlag 1988).

Davies D H, Burstein G T, Corrosion 36, (1980): p. 416.

Grauer R, "The Corrosion Behaviour of Carbon Steel in Portland Cement", NAGRA Technical Report 88-02E, 1988.

Grauer R, Knecht B, Kreis P and Simpson J P, "Hydrogen Evolution from Corrosion of Iron and Steel in Intermediate Level Waste Repositories", p. 295 in Scientific Basis for Nuclear Waste Management **XIV**, T.A.Abrajano and L.H.Johnson (eds.), 1991.

Grauer R, Knecht B, Kreis P and Simpson J P, Werkstoffe und Korrosion 42, (1991): p. 637.

Greef R, Peat R, Peter L M, Pletcher D and Robinson J, Instrumental Methods in Electrochemistry, (Ellis Horwood, Chichester, 1985), p. 240.

Jelinek J, Neufeld P, Corrosion 38, (1982): p. 98.

Kreis P and Simpson J P, "Hydrogen Gas Generation from the Corrosion of Iron in Cementitious Environments", in Corrosion Problems Related to Nuclear Waste Disposal, European Federation of Corrosion Publication number 7, published by Institute of Materials, 1992.

Kreis P, "Hydrogen Evolution from Corrosion of Iron and Steel in Low/Intermediate Level Waste Repositories", NAGRA Technical Report 91-21, 1991.

Kreysa G and Eckerman R, Dechema Corrosion Handbook, volume 11, Seawater, (Dechema, 1992), p. 192.

Linnenbom V J, J. Electrochem. Soc. 105 (1958): p. 321.

Marsh G P, Taylor K J, Sharland S M, Tasker P W, "An Approach for Evaluating the General and Localised Corrosion of Carbon Steel Containers for Nuclear Waste Disposal", MRS Symposium on Nuclear Waste Management, (Boston, Materials Research Society, 1986).

Nomura K, Ujihira Y, J. Mater. Sci. 19 (1984): p. 2664.

Pourbaix M, de Soubov N, Atlas of Electrochemical Equilibria in Aqueous Solutions, (Houston, TX: NACE, 1974), p. 307.

Schenk R, "Untersuchungen Uber Die Wasserstoffbildung Durch Eisen Korrosion Unter Endlagerbdingungen", NAGRA Technical Report 86-24, 1988.

Seo M, Hultquist G, Grasjo L, Sato N, 10th International Congress on Metallic Corrosion, Paper 231 (1986): p. 481.

Shoesmith D W, Rummery T E, Lee Woon, Owen D G, Power Industry Research 1, (1981): p. 43.

Simpson J P and Weber J, "Hydrogen Evolution from Corrosion in Nuclear Waste Repositories", UK Corrosion '88, 1988, p. 33.

Simpson J P, Schenk R and Knecht B, "Corrosion Rate of Unalloyed Steels and Cast Irons In Reducing Granitic Groundwaters and Chloride Solutions", p. 429 in Scientific Basis for Nuclear Waste Management **IX**, L.Werme (ed.), 1985.

Smellie J A T, Laaksoharju M, Wikberg P, J. Hydrol. 172 (1995): p. 147.

Smellie J A T, Wikberg P, J. Hydrol. 126, (1991): p. 129.

Sykes J M, Riley A M, Mater. Sci. Forum 8, (1986): p. 551.

Turnbull A, Gardner M K, Corros. Sci. 22 (1982): p. 661.

Turnbull A, May A T, Br. Corros. J. 22 (1987): p. 176.